Table 1. Spontaneous *gpt* Mutation Spectra of *gpt* Delta Mice and Rats

	C57BL/6J mouse			SD rat			F344 rat		
	No.	CpG	%	No.	CpG	%	No.	CpG	%
Base substitutions									
Transitions									
G:C → A:T	59	(32)	33.3	39	(22)	43.8	12	(3)	40.0
A:T → G:C	19		10.7	6		6.7	1		3.3
Transversions									
G:C → T:A	31		17.5	18		20.2	5		16.7
G:C → C:G	4		2.3	1		1.1	1		3.3
A:T → T:A	13		7.3	1		1.1	1		3.3
A:T → C:G	11		6.2	2		2.2	1		3.3
Deletions	24		13.6	15		16.9	9		30.0
1 bp	18			12			5		
> 2 bps	6			3			4		
Insertions	10		5.6	7		7.9	0		0.0
Others[a)]	6		3.4	0		0.0	0		0.0
Total No. of Mutations	177		100.0	89		100.0	30		100.0
No. of animal	23			31			10		
Sex	male			male and female			male		
Tissues	liver			liver, kidney, mammary gland			liver		
Age	10–20 weeks old			10–52 weeks old			20–24 weeks old		

a) Multiple base substitutions, bese substitutions coupled with deletion or insertion.

lacI transgene.[42,43] De Boer *et al.* reported the spontaneous *lacI* mutations for liver, spleen, bladder, stomach, kidney, bone marrow, lung and skin of Big Blue mice. They showed the similarity of the *lacI* mutational spectra in all tissues.[42] Basically, the predominant class of spontaneous mutations was G:C to A:T transitions, most of which occurred at CpG sites. The second most common class was G:C to T:A transversions. All other base substitution classes contributed less than 10% each. Of the non-base substitution events, the loss of a single base pair was the most frequently occurring event. Zhang *et al.* compared *lacI* spontaneous mutation spectra in the liver of C57BL/6, B6C3F1 and BC-1 mice and F344 rats and concluded that spontaneous mutations appear to be similar, regardless of genetic location, rodent strain, or species.[43]

In sequence analysis of the *gpt* gene recovered from *gpt* delta rats, we should note that an unexpected A:T to T:A transversions at position 299 (*e.g.* nucleotide 299 from the first codon of ATG, in the *gpt* sequence) was frequently observed. We conclude that this base substitution must have arisen in the lambda EG10 DNA during SD rats transgenesis, and is not induced by spontaneous or induced somatic mutagenesis. Evidence for this includes: (1) base substation is observed in untreated rats as well as mutagen-treated rats at a similar frequency; (2) it typically occurs along with another mutation in any given *gpt* mutant; (3) it was detected in gpt^+ (6-TG sensitive) colonies rescued from both *gpt* delta SD and F344 rats; (4) we observed that 96/473 (20%) *gpt* mutants recovered from *gpt* delta rats contain this base substitution [the frequency should be about 20% (2×10^{-1}) if one of five copies of integrated lambda EG10 has A:T to T:A change at position 299]; and (5) it was never found among 1680 *gpt* mutants we have analyzed in *gpt* delta mice. Thus, an A:T to T:A transversion at position 299 observed only in *gpt* delta transgenic rats is a "false" mutation. In the development of transgenic rodents, multiple copy transgenes are usually integrated at a single site of chromosome in a head-to-tail fashion. We suppose that an unintended point mutation might have been arisen in one copy of the transgenes during the first round of DNA replication when they integrated into the chromosome of *gpt* delta SD rat. Although this *gpt* mutation results in an amino acid substitution from isoleucine (Ile) to asparagine (Asn), it doesn't cause a mutated *gpt* phenotype (*e.g.* is a silent mutation) and therefore doesn't affect the *gpt* MF. Because of this, A:T to T:A mutations at 299 were excluded from the mutation spectra of *gpt* delta rats in Table 1.

Table 2. Spontaneous Spi⁻ Mutation Spectra of *gpt* Delta Mice and Rats

	C57BL/6J mouse		SD rat		F344 rat	
	No.	(%)	No.	(%)	No.	(%)
One bp deletions	95	70.4	5	50.0	30	76.9
GGGG	21	15.6	2	20.0	12	30.8
GGG	4	3.0	0	0.0	2	5.1
GG	6	4.4	0	0.0	2	5.1
G	10	7.4	1	10.0	3	7.7
AAAAAA	18	13.3	0	0.0	2	5.1
AAAAA	29	21.5	2	20.0	8	20.5
AAA	1	0.7	0	0.0	1	2.6
AA	0	0.0	0	0.0	0	0.0
A	6	4.4	0	0.0	0	0.0
> 2 bp deletions	28	20.7	2	20.0	4	10.3
2 bps–1 kb	8	5.9	1	10.0	1	2.6
> 1 kb	20	14.8	1	10.0	3	7.7
Complex	6	4.4	1	10.0	5	12.8
Others[a)]	6	4.4	2	20.0	0	0.0
Total No. of Mutations	135	100.0	10	100.0	39	100.0
No. of animal	43		3		10	
Sex	male and female		male		male	
Tissues	brain, colon, liver, bone marrow, epidermis, lung		liver		liver, kidney	
Age	10–20 weeks old		24 weeks old		17–30 weeks old	

a) Deletions coupled with insertions and/or base substitutions.

SPI⁻ ASSAY (SPI⁻ SELECTION) FOR DELETIONS

The Spi⁻ assay is a unique selection that can detect deletions, rather than base substitution mutations. The methodology and the characteristics of the chemical- and radiation-induced Spi⁻ mutations have been described in detail.[1,14] Spi⁻ selection takes advantage of the restricted growth of wild type lambda phage in P2 lysogens.[44] This phenotype is called Spi (sensitive to P2 interference). Only mutant lambda phages that are deficient in the functions of both the *gam* and *red* genes can grow in P2 lysogens and display the Spi⁻ phenotype. Simultaneous inactivation of both the *gam* and *red* genes is usually induced by deletions. Because of the size limitation for *in vitro* packaging reactions (there must be two cos sites separated by 38–51 kb of DNA), the size of deletions detectable by Spi⁻ selection is up to 10 kb. Thus, the mutants are mostly intrachromosomal deletions. However, the tandem array of 80 copies of lambda EG10 DNA in the *gpt* delta mouse provides a potential target of approximately 3.8 megabases.

In previous reports, the spontaneous Spi⁻ MFs of *gpt* delta mice were around $1–5 \times 10^{-6}$, which is lower than that of other transgenes, such as *lacZ* of Muta mice and *lacI* of Big Blue mice. Because the predominant types of point mutations induced *in vivo* are base substitutions, it could be that the spontaneous Spi⁻ MF, which only detects deletion mutations but not base substitutions, is generally lower than that of *lacZ*, *lacI* or *gpt* MF. Tissue type and sex differences of spontaneous Spi⁻ MFs is not clearly observed,[11] although the number of studies in which multiple tissue types have been compared is very limited. The effect of age has not been well characterized. No significant differences in spontaneous MFs were reported in *p53*, *Atm* or *Parp-1* knockout *gpt* delta mice, although heavy-ion or X-ray irradiation induced more large deletions in knockout mice than in wild type mice.[17,21,26] In the *gpt* delta rat, the spontaneous Spi⁻ MFs we have obtained from 13 rat tissues were between 1.3×10^{-6} and 4.4×10^{-6}, similar to those observed in *gpt* delta mice.[12] No marked strain difference has been observed between SD and F344 rats although additional studies are needed to confirm this finding.

Spontaneous Spi⁻ mutation spectra of *gpt* delta rodents are shown in Table 2. Although the sample sizes of the rats are small, mutational characteristics of spontaneous Spi⁻ mutants are similar between

mice and rats. We have analyzed 135, 10 and 39 Spi$^-$ mutants detected in 43 C57BL/6J mice, 3 SD and 10 F344 rats, respectively. These mutants were rescued from brain, liver, epidermis, bone marrow, colon, lung and kidney (and unpublished data in our laboratory).[16,19,20,28,45] The most frequent mutation is a 1 bp deletion in the repetitive sequences in the *gam* gene. These small deletions are not supposed to induce Spi$^-$ mutations. However, translation of the *gam* and *red* genes is probably linked, and the *gam* gene is first transcribed so that the 1 bp deletions in the *gam* gene may interfere with the start of translation of the downstream *red* gene, thereby functionally inactivating not only *gam* but also *red*.[13] The percentages of the 1 bp deletions are from 50–77%. But these values may be underestimated because we regard identical mutations recovered from the same tissue samples to have resulted from clonal expansion and count them as a single mutation. However, they could also be independent hot spot mutations. If this is the case, they should be counted as multiple independent mutations. Indeed, there are several hot spots of spontaneously occurring Spi$^-$ mutations. Those hot spots are 1-bp deletions of AAAAAA to AAAAA at position 295–300, AAAAA to AAAA at 227–231, GGGG to GGG at 286–289, and CCCC to CCC at 238–241 in the *gam* gene (the number starts from the first ATG of the *gam* gene). We suggest these events are most likely induced by slippage errors of DNA polymerases during DNA replication.

Other than 1 bp deletions, we observed about 20% of the Spi$^-$ mutations are larger deletions more than 2 bps in sizes. In mice, based on the sequence characteristics of the junctions and the neighboring regions, the Spi$^-$ deletions more than 1 kb in size could be classified as either those having junctions exhibiting short homology (1–12 bps) (13/20 = 65%) or those having flush junctions (7/20 = 35%). Deletions with short or no homologous sequences at their junctions have been observed in a number of mutant genes implicated in human diseases, including cancer. About 40% of large deletions in human disorders are characterized by the presence of very short sequence homologies at the breakpoints.[46] We suggest that nonhomologous end-joining (NHEJ) repair plays an important role in the generation of intrachromosomal deletions such as Spi$^-$ mutants.[14] This pathway involves the DNA end-binding heterodimer Ku70/Ku80, DNA-dependent protein kinase catalytic subunit (DNA-PKcs), X-ray repair cross complementing (XRCC)4, and DNA ligase IV.[47,48] Although some of these proteins play an essential role in the maintenance of genome stability and suppression of tumorigenesis, NHEJ also has the potential to induce deletion mutations. If two incompatible ends are generated by DNA double-strand breaks (DSBs), they first have to be converted to ligatable ends by enzymatic processing, which often causes deletions.[49] The middle size Spi$^-$ mutants (2 bps to 1 kb) might be caused by DNA replication error or by NHEJ. We have also detected complex type deletions containing genome rearrangement. This type of the Spi$^-$ mutation is sometime difficult to analyze by DNA sequencing. Other deletions coupled with short insertions at junctions or base substitutions are also observed in spontaneous Spi$^-$ mutations. We did not identify hot spots in the Spi$^-$ large deletions either in untreated or mutagen-treated mice. This may indicate that DSBs are randomly induced in the neutral transgene region. Further work is required to understand the mechanism by which Spi$^-$ deletions are generated.

CONCLUSION REMARK

The human genome is continuously exposed to various exogenous and endogenous DNA damaging agents including reactive oxygen species. To survive and protect the genome against DNA damage, cells employ many repair mechanisms such as mismatch repair, base excision repair, nucleotide excision repair, translesion DNA synthesis, and homologous and non-homologous recombination repair mechanisms. However, some repair mechanisms appear to be involved in error-prone DNA replication process or the induction of genome rearrangements such as deletions. To analyze the various types of *in vivo* mutations, *gpt* delta transgenic rodents were established to detect deletions as well as point mutations. Here we reported the characteristics of the spontaneous *gpt* (point mutations) and Spi$^-$ (deletions) mutations obtained from *gpt* delta mice and rats. The results suggested that the assays permit the efficient and quantitative detection of mutations in various tissues of mice and rats, and analysis of mutations at the molecular level. The spontaneous mutations observed in the tissues of mice and rats included both base substitutions and deletions. The predominant types of mutations are G:C to A:T transitions at 5′-CpG-3′ sites, G:C to T:A transversions, 1 bp deletions at repetitive se-

quences, and larger deletions of more than 1 kb. It suggests that deamination of methylated cytosines at CpG sites, oxidative damage to DNA, such as 8-oxoguanine lesions, slippage errors in DNA replication, and error-prone DSB repair may contribute to spontaneous mutations in the rodents. Further studies are necessary to investigate whether oxidative damage in DNA and dNTPs pool induces base substitutions and deletions in mammals and to determine the molecular characteristics of such mutations. Accumulative mutations with age might be related to endogenous oxidative stresses. Genome rearrangements associated with oxidative stress are also important in the field of mutagenesis and carcinogenesis. Because oxidation of DNA is often caused indirectly by malnutrition, the relationship between nutrition and genome rearrangements mediated via oxidative stresses could be an important and interesting topic. To investigate the mechanisms of carcinogenesis in target organs, *gpt* delta rat could be useful because most of carcinogenesis studies are undertaken in rats rather than mice. The mouse model is also useful to investigate specific gene function by crossing with gene knockout mice.

Transgenic mutation assays have the ability to evaluate mutagenesis *in vivo* in a broad range of tissues using neutral reporter genes integrated into genome. Recently, Bielas and Loeb reported a method to directly detect random point mutations in genomic and mitochondrial DNA from mouse and human cells.[50–52] This technique, called random mutation capture, is based on gene capture by hybridization with oligonucleotide probes, followed by cleavage by a restriction enzyme and quantification of the non-cleavable mutants by real-time quantitative PCR. Such a direct detection concept could be extended to quantify mutation in any cell types, at different sites in the genome, in coding and non-coding regions. In another approach, Jiang *et al.* systematically examined the mutational spectrum of the entire human genome and categorized regions using 1.8 million human single nucleotide polymorphisms (SNPs).[53] Although the mutational analysis using SNPs is limited to single base substitutions, extensive and comprehensive sequencing analysis may lead to new perspectives on *in vivo* mutagenesis.

Acknowledgement We thank Dr. D. B. Schauer for critically reading the manuscript. The work was supported by Grants-in-Aid for Cancer Research (20S-8) from the Ministry of Health, Labour and Welfare, Crossover Research and basic research from the Ministry of Education, Sports, Culture, Science and Technology, the Japan Health Science Foundation and public hazard research from the Ministry of Environment, Japan.

REFERENCES

1) Nohmi, T., Suzuki, T. and Masumura, K. (2000) Recent advances in the protocols of transgenic mouse mutation assays. *Mutat. Res.*, **455**, 191–215.
2) Heddle, J. A., Dean, S., Nohmi, T., Boerrigter, M., Casciano, D., Douglas, G. R., Glickman, B. W., Gorelick, N. J., Mirsalis, J. C., Martus, H. J., Skopek, T. R., Thybaud, V., Tindall, K. R. and Yajima, N. (2000) *In vivo* transgenic mutation assays. *Environ. Mol. Mutagen.*, **35**, 253–259.
3) Gossen, J. A., de Leeuw, W. J., Tan, C. H., Zwarthoff, E. C., Berends, F., Lohman, P. H., Knook, D. L. and Vijg, J. (1989) Efficient rescue of integrated shuttle vectors from transgenic mice: a model for studying mutations *in vivo*. *Proc. Natl. Acad. Sci. U.S.A.*, **86**, 7971–7975.
4) Kohler, S. W., Provost, G. S., Kretz, P. L., Dycaico, M. J., Sorge, J. A. and Short, J. M. (1990) Development of a short-term, *in vivo* mutagenesis assay: the effects of methylation on the recovery of a lambda phage shuttle vector from transgenic mice. *Nucleic. Acids. Res.*, **18**, 3007–3013.
5) Kohler, S. W., Provost, G. S., Fieck, A., Kretz, P. L., Bullock, W. O., Sorge, J. A., Putman, D. L. and Short, J. M. (1991) Spectra of spontaneous and mutagen-induced mutations in the *lacI* gene in transgenic mice. *Proc. Natl. Acad. Sci. U.S.A.*, **88**, 7958–7962.
6) Jakubczak, J. L., Merlino, G., French, J. E., Muller, W. J., Paul, B., Adhya, S. and Garges, S. (1996) Analysis of genetic instability during mammary tumor progression using a novel selection-based assay for *in vivo* mutations in a bacteriophage lambda transgene target. *Proc. Natl. Acad. Sci. U.S.A.*, **93**, 9073–9078.
7) Dycaico, M. J., Provost, G. S., Kretz, P. L., Ransom, S. L., Moores, J. C. and Short, J. M. (1994) The use of shuttle vectors for mutation analysis in transgenic mice and rats. *Mutat. Res.*, **307**, 461–478.
8) Suzuki, T., Hayashi, M., Sofuni, T. and Myhr, B. C. (1993) The concomitant detection of gene mutation and micronucleus induction by mitomycin C *in vivo* using *lacZ* transgenic mice. *Mutat. Res.*, **285**, 219–224.
9) Tao, K. S., Urlando, C. and Heddle, J. A. (1993)

Comparison of somatic mutation in a transgenic versus host locus. *Proc. Natl. Acad. Sci. U.S.A*, **90**, 10681–10685.

10) Nohmi, T., Katoh, M., Suzuki, H., Matsui, M., Yamada, M., Watanabe, M., Suzuki, M., Horiya, N., Ueda, O., Shibuya, T., Ikeda, H. and Sofuni, T. (1996) A new transgenic mouse mutagenesis test system using Spi$^-$ and 6-thioguanine selections. *Environ. Mol. Mutagen.*, **28**, 465–470.
11) Masumura, K., Matsui, K., Yamada, M., Horiguchi, M., Ishida, K., Watanabe, M., Ueda, O., Suzuki, H., Kanke, Y., Tindall, K. R., Wakabayashi, K., Sofuni, T. and Nohmi, T. (1999) Mutagenicity of 2-amino-1-methyl-6-phenylimidazo[4,5-*b*]pyridine (PhIP) in the new *gpt* delta transgenic mouse. *Cancer Lett.*, **143**, 241–244.
12) Hayashi, H., Kondo, H., Masumura, K., Shindo, Y. and Nohmi, T. (2003) Novel transgenic rat for *in vivo* genotoxicity assays using 6-thioguanine and Spi$^-$ selection. *Environ. Mol. Mutagen.*, **41**, 253–259.
13) Nohmi, T., Suzuki, M., Masumura, K., Yamada, M., Matsui, K., Ueda, O., Suzuki, H., Katoh, M., Ikeda, H. and Sofuni, T. (1999) Spi(−) selection: An efficient method to detect gamma-ray-induced deletions in transgenic mice. *Environ. Mol. Mutagen.*, **34**, 9–15.
14) Nohmi, T. and Masumura, K. (2005) Molecular nature of intrachromosomal deletions and base substitutions induced by environmental mutagens. *Environ. Mol. Mutagen.*, **45**, 150–161.
15) Masumura, K., Matsui, M., Katoh, M., Horiya, N., Ueda, O., Tanabe, H., Yamada, M., Suzuki, H., Sofuni, T. and Nohmi, T. (1999) Spectra of *gpt* mutations in ethylnitrosourea-treated and untreated transgenic mice. *Environ. Mol. Mutagen.*, **34**, 1–8.
16) Masumura, K., Kuniya, K., Kurobe, T., Fukuoka, M., Yatagai, F. and Nohmi, T. (2002) Heavy-ion-induced mutations in the *gpt* delta transgenic mouse: comparison of mutation spectra induced by heavy-ion, X-ray, and gamma-ray radiation. *Environ. Mol. Mutagen.*, **40**, 207–215.
17) Yatagai, F., Kurobe, T., Nohmi, T., Masumura, K., Tsukada, T., Yamaguchi, H., Kasai-Eguchi, K. and Fukunishi, N. (2002) Heavy-ion-induced mutations in the *gpt* delta transgenic mouse: effect of *p53* gene knockout. *Environ. Mol. Mutagen.*, **40**, 216–225.
18) Horiguchi, M., Masumura, K., Ikehata, H., Ono, T., Kanke, Y., Sofuni, T. and Nohmi, T. (1999) UVB-induced *gpt* mutations in the skin of *gpt* delta transgenic mice. *Environ. Mol. Mutagen.*, **34**, 72–79.
19) Takeiri, A., Mishima, M., Tanaka, K., Shioda, A., Ueda, O., Suzuki, H., Inoue, M., Masumura, K. and Nohmi, T. (2003) Molecular characterization of mitomycin C-induced large deletions and tandem-base substitutions in the bone marrow of *gpt* delta transgenic mice. *Chem. Res. Toxicol.*, **16**, 171–179.
20) Masumura, K., Matsui, K., Yamada, M., Horiguchi, M., Ishida, K., Watanabe, M., Wakabayashi, K. and Nohmi, T. (2000) Characterization of mutations induced by 2-amino-1-methyl-6-phenylimidazo[4,5-*b*]pyridine in the colon of *gpt* delta transgenic mouse: novel G:C deletions beside runs of identical bases. *Carcinogenesis*, **21**, 2049–2056.
21) Furuno-Fukushi, I., Masumura, K., Furuse, T., Noda, Y., Takahagi, M., Saito, T., Hoki, Y., Suzuki, H., Wynshaw-Boris, A., Nohmi, T. and Tatsumi, K. (2003) Effect of *Atm* disruption on spontaneously arising and radiation-induced deletion mutations in mouse liver. *Radiat. Res.*, **160**, 549–558.
22) Masumura, K., Horiguchi, M., Nishikawa, A., Umemura, T., Kanki, K., Kanke, Y. and Nohmi, T. (2003) Low dose genotoxicity of 2-amino-3,8-dimethylimidazo[4,5-*f*]quinoxaline (MeIQx) in *gpt* delta transgenic mice. *Mutat. Res.*, **541**, 91–102.
23) Masumura, K., Totsuka, Y., Wakabayashi, K. and Nohmi, T. (2003) Potent genotoxicity of aminophenylnorharman, formed from non-mutagenic norharman and aniline, in the liver of *gpt* delta transgenic mouse. *Carcinogenesis*, **24**, 1985–1993.
24) Kanki, K., Nishikawa, A., Masumura, K., Umemura, T., Imazawa, T., Kitamura, Y., Nohmi, T. and Hirose, M. (2005) *In vivo* mutational analysis of liver DNA in *gpt* delta transgenic rats treated with the hepatocarcinogens *N*-nitrosopyrrolidine, 2-amino-3-methylimidazo[4,5-*f*]quinoline, and di(2-ethylhexyl)phthalate. *Mol. Carcinog.*, **42**, 9–17.
25) Hashimoto, A. H., Amanuma, K., Hiyoshi, K., Takano, H., Masumura, K., Nohmi, T. and Aoki, Y. (2005) *In vivo* mutagenesis induced by benzo[*a*]pyrene instilled into the lung of *gpt* delta transgenic mice. *Environ. Mol. Mutagen.*, **45**, 365–373.
26) Shibata, A., Kamada, N., Masumura, K., Nohmi, T., Kobayashi, S., Teraoka, H., Nakagama, H., Sugimura, T., Suzuki, H. and Masutani, M. (2005) *Parp-1* deficiency causes an increase of deletion mutations and insertions/rearrangements *in vivo* after treatment with an alkylating agent. *Oncogene*, **24**, 1328–1337.
27) Miyazaki, M., Yamazaki, H., Takeuchi, H., Saoo, K., Yokohira, M., Masumura, K., Nohmi, T.,

Funae, Y., Imaida, K. and Kamataki, T. (2005) Mechanisms of chemopreventive effects of 8-methoxypsoralen against 4-(methylnitrosamino)-1-(3-pyridyl)-1-butanone-induced mouse lung adenomas. *Carcinogenesis*, **26**, 1947-1955.

28) Ikeda, M., Masumura, K., Sakamoto, Y., Wang, B., Nenoi, M., Sakuma, K., Hayata, I. and Nohmi, T. (2007) Combined genotoxic effects of radiation and a tobacco-specific nitrosamine in the lung of *gpt* delta transgenic mice. *Mutat. Res.*, **626**, 15–25.

29) Ono, T., Miyamura, Y., Ikehata, H., Yamanaka, H., Kurishita, A., Yamamoto, K., Suzuki, T., Nohmi, T., Hayashi, M. and Sofuni, T. (1995) Spontaneous mutant frequency of *lacZ* gene in spleen of transgenic mouse increases with age. *Mutat. Res.*, **338**, 183–188.

30) Sutherland, B. M., Bennett, P. V., Sidorkina, O. and Laval, J. (2000) Clustered DNA damages induced in isolated DNA and in human cells by low doses of ionizing radiation. *Proc. Natl. Acad. Sci. U.S.A.*, **97**, 103–108.

31) de Vries, A., Dolle, M. E., Broekhof, J. L., Muller, J. J., Kroese, E. D., van Kreijl, C. F., Capel, P. J., Vijg, J. and van Steeg, H. (1997) Induction of DNA adducts and mutations in spleen, liver and lung of XPA-deficient/*lacZ* transgenic mice after oral treatment with benzo[*a*]pyrene: correlation with tumour development. *Carcinogenesis*, **18**, 2327–2332.

32) Dolle, M. E., Snyder, W. K., Gossen, J. A., Lohman, P. H. and Vijg, J. (2000) Distinct spectra of somatic mutations accumulated with age in mouse heart and small intestine. *Proc. Natl. Acad. Sci. U.S.A.*, **97**, 8403–8408.

33) Lee, A. T., DeSimone, C., Cerami, A. and Bucala, R. (1994) Comparative analysis of DNA mutations in *lacI* transgenic mice with age. *FASEB J.*, **8**, 545–550.

34) Stuart, G. R., Oda, Y., de Boer, J. G. and Glickman, B. W. (2000) Mutation frequency and specificity with age in liver, bladder and brain of *lacI* transgenic mice. *Genetics*, **154**, 1291–1300.

35) Hill, K. A., Buettner, V. L., Halangoda, A., Kunishige, M., Moore, S. R., Longmate, J., Scaringe, W. A. and Sommer, S. S. (2004) Spontaneous mutation in Big Blue mice from fetus to old age: tissue-specific time courses of mutation frequency but similar mutation types. *Environ. Mol. Mutagen.*, **43**, 110–120.

36) Minowa, O., Arai, T., Hirano, M., Monden, Y., Nakai, S., Fukuda, M., Itoh, M., Takano, H., Hippou, Y., Aburatani, H., Masumura, K., Nohmi, T., Nishimura, S. and Noda, T. (2000) *Mmh/Ogg1* gene inactivation results in accumulation of 8-hydroxyguanine in mice. *Proc. Natl. Acad. Sci. U.S.A.*, **97**, 4156–4161.

37) Sato, Y., Takahashi, S., Kinouchi, Y., Shiraki, M., Endo, K., Matsumura, Y., Kakuta, Y., Tosa, M., Motida, A., Abe, H., Imai, G., Yokoyama, H., Nomura, E., Negoro, K., Takagi, S., Aihara, H., Masumura, K., Nohmi, T. and Shimosegawa, T. (2006) IL-10 deficiency leads to somatic mutations in a model of IBD. *Carcinogenesis*, **27**, 1068–1073.

38) Aoki, Y., Hashimoto, A. H., Amanuma, K., Matsumoto, M., Hiyoshi, K., Takano, H., Masumura, K., Itoh, K., Nohmi, T. and Yamamoto, M. (2007) Enhanced spontaneous and benzo(*a*)pyrene-induced mutations in the lung of Nrf2-deficient *gpt* delta mice. *Cancer Res.*, **67**, 5643–5648.

39) Bird, A. P. (1986) CpG-rich islands and the function of DNA methylation. *Nature*, **321**, 209–213.

40) Moriya, M. (1993) Single-stranded shuttle phagemid for mutagenesis studies in mammalian cells: 8-oxoguanine in DNA induces targeted G.C→T.A transversions in simian kidney cells. *Proc. Natl. Acad. Sci. U.S.A.*, **90**, 1122–1126.

41) Sagher, D. and Strauss, B. (1983) Insertion of nucleotides opposite apurinic/apyrimidinic sites in deoxyribonucleic acid during *in vitro* synthesis: uniqueness of adenine nucleotides. *Biochemistry*, **22**, 4518–4526.

42) de Boer, J. G., Provost, S., Gorelick, N., Tindall, K. and Glickman, B. W. (1998) Spontaneous mutation in *lacI* transgenic mice: a comparison of tissues. *Mutagenesis*, **13**, 109–114.

43) Zhang, S., Glickman, B. W. and de Boer, J. G. (2001) Spontaneous mutation of the *lacI* transgene in rodents: absence of species, strain, and insertion-site influence. *Environ. Mol. Mutagen.*, **37**, 141–146.

44) Ikeda, H., Shimizu, H., Ukita, T. and Kumagai, M. (1995) A novel assay for illegitimate recombination in *Escherichia coli*: stimulation of lambda bio transducing phage formation by ultra-violet light and its independence from RecA function. *Adv. Biophys.*, **31**, 197–208.

45) Horiguchi, M., Masumura, K., Ikehata, H., Ono, T., Kanke, Y. and Nohmi, T. (2001) Molecular nature of ultraviolet B light-induced deletions in the murine epidermis. *Cancer Res.*, **61**, 3913–3918.

46) Morris, T. and Thacker, J. (1993) Formation of large deletions by illegitimate recombination in the HPRT gene of primary human fibroblasts. *Proc. Natl. Acad. Sci. U.S.A.*, **90**, 1392–1396.

47) Kanaar, R., Hoeijmakers, J. H. and van Gent, D. C. (1998) Molecular mechanisms of DNA double

strand break repair. *Trends Cell Biol.*, **8**, 483–489.
48) van Gent, D. C., Hoeijmakers, J. H. and Kanaar, R. (2001) Chromosomal stability and the DNA double-stranded break connection. *Nat. Rev. Genet.*, **2**, 196–206.
49) Feldmann, E., Schmiemann, V., Goedecke, W., Reichenberger, S. and Pfeiffer, P. (2000) DNA double-strand break repair in cell-free extracts from Ku80-deficient cells: implications for Ku serving as an alignment factor in non-homologous DNA end joining. *Nucleic Acids Res.*, **28**, 2585–2596.
50) Bielas, J. H. and Loeb, L. A. (2005) Quantification of random genomic mutations. *Nature Methods*, **2**, 285–290.
51) Bielas, J. H., Loeb, K. R., Rubin, B. P., True, L. D. and Loeb, L. A. (2006) Human cancers express a mutator phenotype. *Proc. Natl. Acad. Sci. U.S.A.*, **103**, 18238–18242.
52) Vermulst, M., Bielas, J. H., Kujoth, G. C., Ladiges, W. C., Rabinovitch, P. S., Prolla, T. A. and Loeb, L. A. (2007) Mitochondrial point mutations do not limit the natural lifespan of mice. *Nat. Genet.*, **39**, 540–543.
53) Jiang, C. and Zhao, Z. (2006) Mutational spectrum in the recent human genome inferred by single nucleotide polymorphisms. *Genomics*, **88**, 527–534.

Mutation Research xxx (2009) xxx–xxx

Contents lists available at ScienceDirect

Mutation Research/Fundamental and Molecular Mechanisms of Mutagenesis

journal homepage: www.elsevier.com/locate/molmut
Community address: www.elsevier.com/locate/mutres

Role of Parp-1 in suppressing spontaneous deletion mutation in the liver and brain of mice at adolescence and advanced age

Atsushi Shibata[a,b,c], Daisuke Maeda[a,b], Hideki Ogino[a,b], Masahiro Tsutsumi[d], Takehiko Nohmi[e], Hitoshi Nakagama[a], Takashi Sugimura[a], Hirobumi Teraoka[c], Mitsuko Masutani[a,b,*]

[a] Biochemistry Division, National Cancer Center Research Institute, Chuo-ku, Tokyo 104-0045, Japan
[b] ADP-ribosylation in Oncology Project, National Cancer Center Research Institute, Chuo-ku, Tokyo 104-0045, Japan
[c] Medical Research Institute, Tokyo Medical and Dental University, Chiyoda-ku, Tokyo 101-0062, Japan
[d] Pathology, Saiseikai Chuwa Hospital, Sakurai-City, Nara 633-0054, Japan
[e] Division of Genetics and Mutagenesis, National Institute of Health Sciences, Setagaya-ku, Tokyo 158-8501, Japan

ARTICLE INFO

Article history:
Received 16 August 2008
Received in revised form 30 January 2009
Accepted 4 February 2009
Available online xxx

Keywords:
Parp-1
Mutation
Deletion
gpt delta
Aging

ABSTRACT

Poly(ADP-ribose) polymerase-1 knockout (*Parp-1*$^{-/-}$) mice show increased frequency of spontaneous liver tumors compared to wild-type mice after aging. To understand the impact of *Parp-1* deficiency on mutations during aging, in this study, we analyzed spontaneous mutations in *Parp-1*$^{-/-}$ aged mice. *Parp-1*$^{-/-}$ mice showed tendencies of higher mutation frequencies of the *red/gam* genes at 18 months of age, compared to *Parp-1*$^{+/+}$ mice, in the liver and brain. Complex-type deletions, accompanying small insertion were observed only in *Parp-1*$^{-/-}$ mice in the liver and brain. Further analysis in the liver showed that the frequency of single base deletion mutations at non-repeat or short repeat sequences was 5.8-fold higher in *Parp-1*$^{-/-}$ than in *Parp-1*$^{+/+}$ mice ($p < 0.05$). A 3.2-fold higher tendency of the deletion frequency of two bases or more was observed in *Parp-1*$^{-/-}$ mice compared to *Parp-1*$^{+/+}$ mice ($p = 0.084$). These results support the model that *Parp-1* is involved in suppressing imprecise repair of endogenous DNA damage leading to deletion mutation during aging. The mutation frequencies of the *gpt* gene in the brain were found to be 3-fold lower in *Parp-1*$^{-/-}$ than in *Parp-1*$^{+/+}$ mice at 4 months of age ($p < 0.01$), implying that Parp-1 may be positively involved in imprecise DNA repair in the brain. On the other hand, the frequencies of *gpt* mutation showed an increase at 18 months of age in the *Parp-1*$^{-/-}$ ($p < 0.05$) but not in *Parp-1*$^{+/+}$ brains, suggesting that *Parp-1* deficiency causes an increase of point mutations in the brain by aging.

1. Introduction

Poly(ADP-ribose) polymerase-1 (Parp-1) facilitates DNA strand break repair by binding to the end of DNA strand breaks and catalyzing transfer of ADP-ribose residues from NAD to itself and other nuclear proteins, including XRCC1 (X-ray cross-complementing factor 1) [1], WRN (Werner's syndrome protein) [2,3] and Ku70/80 [4,5]. PolyADP-ribosylation results in recruitment of DNA repair proteins to DNA damage sites [6,7]. Accumulating studies have indicated that Parp-1 is involved in base excision repair (BER) and single strand break (SSB) repair by interacting with XRCC1 through poly(ADP-ribose) residues, as well as DNA polymerase β [8] and DNA ligase IIIα [9] using the BRCT domain in Parp-1. We previously demonstrated that *Parp-1*$^{-/-}$ mice show higher susceptibility to carcinogenesis induced by alkylating agents such as *N*-nitrosobis(2-hydroxypropyl)amine (BHP) [10] and azoxymethane [11] but not with 4-nitroquinoline 1-oxide [12]. *Parp-1*$^{-/-}$ mice develop normally, and spontaneous tumor incidences in all organs are not elevated at least until 9 months old [11]. However, the incidences of hepatocellular adenomas and carcinomas in *Parp-1*$^{-/-}$ mice are increased at 18–24 months old compared to *Parp-1*$^{+/+}$ mice [13]. *Parp-1*$^{-/-}$*p53*$^{-/-}$ mice also show spontaneous medulloblastomas in *p53* knockout (*p53*$^{-/-}$) mice at a higher incidence compared to *Parp-1*$^{+/+}$*p53*$^{-/-}$ mice [14,15].

In wild-type mice, age-related increases of mutant frequencies are observed in the liver, spleen, heart and small intestine, whereas mutant frequencies in the brain and germ cells are only slightly increased [16–18]. Age-related increases in genome rearrangement as well as point mutations are reported in the liver but not observed in the brain [19]. Therefore, the effects of aging on spontaneous mutation frequency might be different among tissues.

To analyze the impact of aging on spontaneous mutant frequency and its spectra in *Parp-1*$^{-/-}$ mice, we performed mutation analysis in *Parp-1*$^{-/-}$ mice at advanced age using progeny of

* Corresponding author at: Biochemistry Division, National Cancer Center Research Institute, 5-1-1, Chuo-ku, Tokyo 104-0045, Japan. Tel.: +81 3 3542 2511; fax: +81 3 3542 2530.
E-mail address: mmasutan@ncc.go.jp (M. Masutani).

0027-5107/$ – see front matter © 2009 Elsevier B.V. All rights reserved.
doi:10.1016/j.mrfmmm.2009.02.001

intercross with *gpt* delta transgenic mice harboring about 80 copies of tandemly integrated lambda EG10 DNA as a transgene [20,21]. The rescued phage was analyzed by the Spi$^-$ (sensitive to P2 interference) assay, which preferentially detects deletion mutations in the *red/gam* genes. The deletion mutations of a single base to approximately 10 kb or several copies of EG10 DNA could be detected. The *gpt* assay detects point mutations in the guanine phosphoribosyl transferase (*gpt*) gene. The spontaneous mutant frequency of the *gpt* gene in the liver of mice is around $2–6 \times 10^{-6}$ [23] in tissues including the liver and brain [24]. The frequency of mutation in the *red/gam* genes in the liver of mice is also reported to be around $1–5 \times 10^{-6}$ [23,24].

Analysis of deletion mutation with a Spi$^-$ assay using *gpt* delta transgenic mice has been shown to be useful in detecting deletion mutations after treatment with various types of chemicals or irradiation with γ-rays or heavy ions [23,25–26].

The results in this study suggest that Parp-1 suppresses spontaneous deletion mutations, especially at non-repeat or short repeat sequences in the liver and brain during aging. Complex-type deletions accompanying small insertion and microhomology at deletion junctions observed in *Parp-1*$^{-/-}$ livers and brains are also discussed. Additionally, we observed that the mutant frequencies of the *gpt* gene in the brains were found to be 3-fold lower in *Parp-1*$^{-/-}$ than in *Parp-1*$^{+/+}$ mice at 4 months of age but increased in *Parp-1*$^{-/-}$ mice to the level of *Parp-1*$^{+/+}$ mice at 18 months of age.

2. Materials and methods

2.1. Genomic DNA extraction and rescue of the transgene

Parp-1$^{-/-}$/*gpt* delta and *Parp-1*$^{+/+}$/*gpt* delta animals were previously established by intercrossing *Parp-1*$^{+/-}$/*gpt* delta mice [20]. The mice possess mixed genetic background of C57BL/6, ICR and 129Sv. Male *Parp-1*$^{-/-}$ and *Parp-1*$^{+/+}$ mice were fed a basal diet (CE-2, Clea Japan), and these mice were anaesthetized and sacrificed at the ages of 4 months ($n = 5$ for each genotype) and 18 months ($n = 6$ (*Parp-1*$^{-/-}$) and $n = 4$ (*Parp-1*$^{+/+}$)). The livers and brains were immediately frozen in liquid nitrogen, and stored at −80 °C until DNA extraction. Genomic DNA was extracted by a RecoverEase DNA isolation kit (Stratagene). Two out of six *Parp-1*$^{-/-}$ mice (mouse ID, G60 and G94) of 18 months of age harbored tumors in the liver, and genomic DNA was extracted from areas containing no tumors. A lambda phage *in vitro* packaging reaction was performed with Transpack Packaging Extract (Stratagene). Part of the tissues were also fixed with formalin solution, routinely processed and sections were stained with hematoxyline-eosine. The experimental protocol was approved by the Ethics Review Committee for Animal Experimentation of the National Cancer Center Research Institute.

2.2. Spi$^-$ assay

A Spi$^-$ assay [21] was carried out with a modification as described previously [27]. The frequencies of background mutants were less than 10^{-8} in the Spi$^-$ assay and were negligible [28]. The data for Spi$^-$ mutant frequencies were therefore presented without subtracting the background mutant frequencies. To narrow down the deleted region, the structure of each mutation was analyzed by a Southern blot hybridization method that uses oligonucleotide DNA probes [29]. DNA sequencing of the mutated region was performed with a CEQ™ DTCS Quick Start Kit (Beckman Coulter).

2.3. gpt assay

The *gpt* assay was performed as described previously [21]. Briefly, the phages rescued from genomic DNA were transfected into *E. coli* YG6020 expressing Cre recombinase. Infected cells were cultured at 37 °C on plates containing chloramphenicol (Cm) and 6-thioguanine (6-TG) for 3 days until 6-TG resistant colonies appeared. To confirm the 6-TG resistant phenotype, colonies were restreaked on plates containing Cm and 6-TG. A 739 bp DNA fragment encompassing the *gpt* gene was amplified by PCR [30]. DNA sequencing of the target 456 bp in the *gpt* gene was performed with a CEQ™ DTCS Quick Start Kit (Beckman Coulter).

2.4. Statistical analysis

The statistical significance of differences in mutant or mutation frequencies between the two groups was analyzed by using the Mann–Whitney *U* test. When *p* value is less than 0.05, the difference was considered significant. Because the individual differences in mutant frequency became larger at advanced ages, "tendency of ≥1.5 fold increase or reduction" in the mutant frequency is also mentioned with *p* value in the text, when *p* value is equal to or larger than 0.05.

3. Results

3.1. Analysis of spontaneous mutant frequency of the red/gam genes and the gpt genes in the livers of Parp-1$^{-/-}$ mice at 4 and 18 months of age

There was no difference in the mutant frequencies of the *red/gam* genes in the liver between *Parp-1*$^{-/-}$ and *Parp-1*$^{+/+}$ mice at 4 months of age. The liver of *Parp-1*$^{-/-}$ mice at 18 months of age showed a 1.7-fold higher tendency of the *red/gam* mutant frequencies than those in *Parp-1*$^{+/+}$ mice ($p = 0.34$, Fig. 1A). The tendency of age-dependent 1.5-fold increase in mutant frequency was observed in *Parp-1*$^{-/-}$ but not in *Parp-1*$^{+/+}$ mice.

On the other hand, in the case of the *gpt* gene (Fig. 1B), in which point mutations are mostly detected, the mutant frequencies in *Parp-1*$^{+/+}$ mice showed a higher elevation at 18 months than that at 4 months ($p = 0.037$). In *Parp-1*$^{-/-}$ mice, a tendency of higher mutant frequency was noticed at 18 months compared to that at 4 months ($p = 0.14$). There was no significant difference in the mutant frequency of *gpt* gene between *Parp-1*$^{-/-}$ and *Parp-1*$^{+/+}$ mice at either 4 or 18 months (Fig. 1B).

3.2. Structural analysis of deletion mutations in the red/gam genes of Parp-1$^{-/-}$ mice at 18 months of age

The mutations in the *red/gam* genes could be categorized into deletion, base substitution and single base insertion. As shown in Fig. 1C, deletion mutation frequencies in the liver of *Parp-1*$^{-/-}$ mice showed a tendency of 1.7-fold increase compared to those in *Parp-1*$^{+/+}$ mice ($p = 0.20$). The deletion mutations could be classified into single base deletion and deletion of two bases or more (Fig. 1C). Fig. 1D shows the distribution of single base deletions of the *gam* gene in the liver of *Parp-1*$^{-/-}$ and *Parp-1*$^{+/+}$ mice at 18 months of age. Single nucleotide repeats, –AAAAA– at 227–231, –AAAAAA– at 295–300 and –GGGG– at 286–289, are known as hot spots of single base deletions in the *gam* gene of wild-type mice [28]. The frequency of single base deletions at hot spots, namely at 4–6 bp mononucleotide repeats was not increased in *Parp-1*$^{-/-}$ mice compared to *Parp-1*$^{+/+}$ mice (Fig. 1C). In contrast, the frequency of single base deletions at non-repeat sequences or short repeats of 2–3 bp mononucleotides showed a 5.8-fold increase in *Parp-1*$^{-/-}$ mice ($p = 0.031$, Fig. 1C). The single base deletions at non-repeat sequences were only observed in *Parp-1*$^{-/-}$ mice at a frequency of 4.3×10^{-7} and showed a higher frequency than that in *Parp-1*$^{+/+}$ mice ($p = 0.023$). The specific deletion mutation frequencies of two bases or more in the liver showed a 3.2-fold (Fig. 1C) higher tendency in *Parp-1*$^{-/-}$ mice than those in *Parp-1*$^{+/+}$ mice, although there was no statistical significance ($p = 0.084$). Deletions of both 2 bp–1 kb and deletions larger than 1 kb were observed in the liver of *Parp-1*$^{-/-}$ mice, whereas all three mutants in *Parp-1*$^{+/+}$ mice (Table 1) had deletions larger than 1 kb (data not shown).

The deletion mutations of two bases or more were also categorized into those that occurred at non-repeat and short repeat sequences of mononucleotides. Frequencies of deletion mutations of two bases or more at non-repeat and short repeats of mononucleotides showed a higher tendency in *Parp-1*$^{-/-}$ than *Parp-1*$^{+/+}$ mice ($p = 0.28$) at 18 months old (Fig. 1C). There was no deletion mutation of two bases or more that occurred on a mononucleotide repeat larger than 4 bp in both genotypes.

We further categorized deletion mutations of two bases or more into simple or complex types (Table 1). Complex-type deletions were defined as accompanying small insertions or recombination with deletions [20]. Complex-type deletions were found in

Please cite this article in press as: A. Shibata, et al., Role of Parp-1 in suppressing spontaneous deletion mutation in the liver and brain of mice at adolescence and advanced age, Mutat. Res.: Fundam. Mol. Mech. Mutagen. (2009), doi:10.1016/j.mrfmmm.2009.02.001

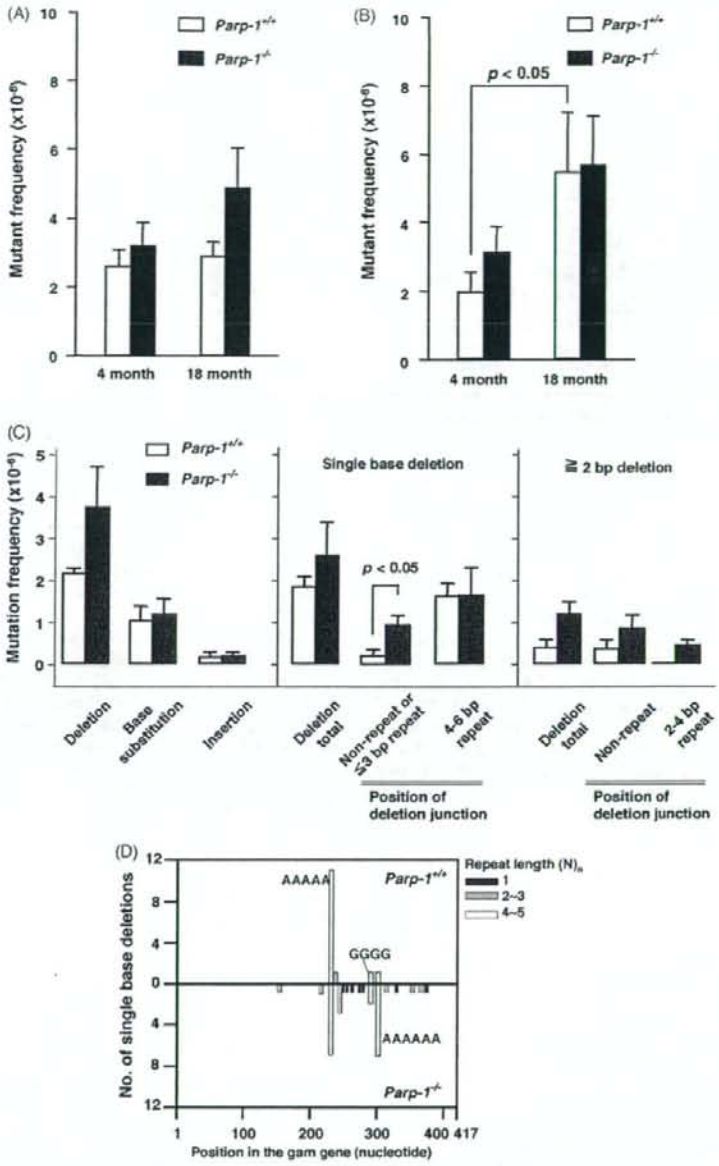

Fig. 1. Spontaneous mutant frequencies of the *red/gam* and *gpt* genes in the liver of *Parp-1*$^{-/-}$ and *Parp-1*$^{+/+}$ mice at 4 and 18 months of age. (A) Spontaneous mutant frequencies of the *red/gam* genes in the livers. (B) Spontaneous mutant frequencies in the *gpt* genes of the livers. Error bars represent standard error values. (C) Effect of *Parp-1* deficiency on the mutation spectrum of the *red/gam* genes in the liver at 18 months of age. Specific mutation frequencies in the *red/gam* genes of the liver are shown. Mean values and standard error values are presented for *Parp-1*$^{-/-}$ and *Parp-1*$^{+/+}$ mice ($n = 6$ and 4, respectively). (D) Distribution of single base deletion mutations in the *gam* gene of the livers at 18 months of age. Single base deletions were observed on non-repeat, or 2–3 base repeats, or 4–6 base repeats as indicated in the figure as repeat length $(N)_n$ of 1, 2, 4–6, respectively.

Parp-1$^{-/-}$ mice, but not in *Parp-1*$^{+/+}$ mice in the liver at 18 months old. As shown in Table 1, the frequencies of complex-type deletions in *Parp-1*$^{-/-}$ mice showed a higher tendency than those in *Parp-1*$^{+/+}$ mice, although it is not statistically significant ($p = 0.224$). The structures of complex-type mutations of *Parp-1*$^{-/-}$ mice observed at 18 months of age are shown in Table 2. Two complex-type deletions observed in *Parp-1*$^{-/-}$ mice accompanied both small insertions and microhomologous sequences at deletion junctions (Table 2). It is of note that complementary nucleotides AAA (G61-1-3) or TT (G93-2-3) (marked with upper lines in Table 2) are present at the 5′ position to these microhomologous deletion junctions in each case.

Please cite this article in press as: A. Shibata, et al., Role of Parp-1 in suppressing spontaneous deletion mutation in the liver and brain of mice at adolescence and advanced age, Mutat. Res.: Fundam. Mol. Mech. Mutagen. (2009), doi:10.1016/j.mrfmmm.2009.02.001

Table 1
Spectrum of the mutations of two bases or more in the *red/gam* genes in the liver and brain of *Parp-1*$^{-/-}$ mice at 18 months old.

Tissue	Deletion	*Parp-1*$^{+/+}$		*Parp-1*$^{-/-}$	
		Mutation frequency ($\times 10^{-6}$)	No. of mutants (MEJ/Non-MEJ)	Mutation frequency ($\times 10^{-6}$)	No. of mutants (MEJ/Non-MEJ)
Liver	Simple	0.34 ± 0.21	3 (2/1)	0.96 ± 0.27	13 (6/7)
	Complex	<0.16	0	0.13 ± 0.08	2 (2/0)
	with small insertion[a]	<0.16	0	0.13 ± 0.08	2 (2/0)
	with recombination	<0.16	0	<0.13	0
Brain	Simple	0.15 ± 0.15	1 (0/1)	0.32 ± 0.14	3 (2/1)
	Complex	<0.18	0	0.32 ± 0.14	3 (1/1)*
	with small insertion	<0.18	0	0.19 ± 0.12	2 (1/1)
	with recombination	<0.18	0	0.12 ± 0.12	1

MEJ; microhomology-mediated end joining. Non-MEJ; non-microhomology-mediated end joining.
[a] Small insertion represents 4–9 bp insertion.
* One of the mutants could not be classified into MEJ or non-MEJ type.

3.3. Mutation frequencies of the red/gam gene in the brains at 4 and 18 months of age

Parp-1$^{-/-}$ mice showed 1.5-fold higher mutant frequencies compared to *Parp-1*$^{+/+}$ mice ($p = 0.047$) in the brains at 4 months of age (Fig. 2A). The brains of *Parp-1*$^{-/-}$ mice showed a 2.2-fold higher tendency of mutant frequencies than those in *Parp-1*$^{+/+}$ mice ($p = 0.088$) at 18 months of age (Fig. 2A). The tendency of age-dependent slight increase in the mutant frequency in the brain was observed in *Parp-1*$^{-/-}$ but not in *Parp-1*$^{+/+}$ mice, as mentioned earlier in the case with the liver. Analysis of the mutation spectrum in the brain (Fig. 2C) revealed some differences from that of the livers. In the brain, a tendency of increase in base substitution and deletion mutations of two bases or more was observed in *Parp-1*$^{-/-}$ mice compared to *Parp-1*$^{+/+}$ mice (base substitution: $p = 0.055$, deletion mutation: $p = 0.11$). Different from the cases in the liver, the frequency of single base deletions at non-repeat or 2–3 bp repeats is not increased in the brain of *Parp-1*$^{-/-}$ mice at 18 months of age compared to *Parp-1*$^{+/+}$ mice (Fig. 2C).

3.4. Lower mutation frequencies of the gpt gene in the brains of Parp-1$^{-/-}$ than Parp-1$^{+/+}$ mice at 4 months of age and age-dependent increase

Of note, mutant frequencies of the *gpt* gene in the brains of *Parp-1*$^{-/-}$ mice were lower than those of *Parp-1*$^{+/+}$ mice ($p = 0.009$) at 4 months of age (Fig. 2B). No pathological changes in the brains were observed in *Parp-1*$^{-/-}$ and *Parp-1*$^{+/+}$ mice. Mutation spectra in the brains of *Parp-1*$^{-/-}$ mice showed a lower frequency of G:C to A:T base transition mutations ($p = 0.047$) as well as deletion mutations ($p = 0.034$) compared to *Parp-1*$^{+/+}$ mice at 4 months old (Fig. 2D).

The *gpt* mutant frequency showed an increase at 18 months of age in the *Parp-1*$^{-/-}$ but not in *Parp-1*$^{+/+}$ mice ($p = 0.011$, Fig. 2B). There was no difference in the mutant frequencies of the *gpt* gene in the brain between *Parp-1*$^{-/-}$ and *Parp-1*$^{+/+}$ mice at 18 months of age (Fig. 2B).

Comparison of the mutation spectra between 4 and 18 months of age in *Parp-1*$^{-/-}$ mice suggests a tendency of age-dependent increase in the frequencies of deletion mutations ($p = 0.068$, Fig. 2D). A tendency of increase of point mutation ($p = 0.144$) is also noticed, suggesting that Parp-1 may be involved in suppressing age-dependent introduction of point mutations in the brain.

4. Discussion

Spontaneous *gpt* and *red/gam* mutant frequencies are reported to be around $2–6 \times 10^{-6}$ and $1–5 \times 10^{-6}$, respectively, in *gpt* delta mice of C57BL/6 genetic background [23,24]. In this study, the spontaneous mutation frequencies of *gpt* and *red/gam* mutant frequencies in the liver and the brain of *Parp-1*$^{+/+}$ are both around 2×10^{-6} at 4 months of age and thus consistent with the previous reports. The mutant frequency of the *gpt* gene in the small intestine

Table 2
Junctional sequences of complex-type mutations in the liver and brain of *Parp-1*$^{-/-}$ mice at 18 months old.

Tissue	Mutant ID[a]	Original sequence in lambdaEG10	Junctional sequence of mutation	Deletion/insertion size (nucleotide position in lambdaEG10)
Liver	G61-1-3	5′-GTCATCAAACgcac tttt**GCT**GGCCCCG-3′ 3′-CAGTAGTTTGcgtg aaaa**CGA**CCGGGGC-5′	5′-GTCATCAAACacac**GCT**GGCCCCG-3′ 3′-CAGTAGTTTGtgtg**CGA**CCGGGGC-5′	20 bp deletion + 4 bp insertion (25021 - 25040)
	G93-2-3	5′-CCGTGGCGTTgcaa ataa**GCG**TTCATGG-3′ 3′-GGCACCGCAAcgtt tatt**CGC**AAGTACC-5′	5′-CCGTGGCGTTttgctg**GCG**TTCATGG-3′ 3′-GGCACCGCAAaacgac**CGC**AAGTACC-5′	149 bp deletion + 6 bp insertion (25058 - 25206)
Brain	G61-1-1	5′-TTCATTAGACttat tagt**GAA**TGCTTTT-3′ 3′-AAGTAATCTGaata atca**CTT**ACGAAAA-5′	5′-TTCATTAGACaaatta**GAA**TGCTTTT-3′ 3′-AAGTAATCTGtttaat**CTT**ACGAAAA-5′	3694 bp deletion + 6 bp insertion (21600 - 25293)
	G94-1-1	5′-TGTCTGCATGgaga aatc**GA**TTTCCCT-3′ 3′-ACAGACGTACctct ttag**CTA**AAAGGGA-5′	5′-TGTCTGCATGagaccaga**GA**TTTTCCCT-3′ 3′-CGTACCTCTGtctggtct**CTA**AAAGGGA-5′	3805 bp deletion + 9 bp insertion (21682 - 25486)
	G93-2-4	acgcGCCCAGCTCT-3′ tgcgCGGGTCGAGA-5′	5′-taagagtcagGCCCAGCTCT-3′ 3′-attctcagtcCGGGTCGAGA-5′	Recombination with unknown sequence

[a] ID; Identification number. Red and blue letters indicate deleted and inserted sequences, respectively. Letters in the box are microhomologous sequences. Upperlines show complementary mononucleotide sequences at 5′ positions of the microhomologous sequences.

Please cite this article in press as: A. Shibata, et al., Role of Parp-1 in suppressing spontaneous deletion mutation in the liver and brain of mice at adolescence and advanced age. Mutat. Res.: Fundam. Mol. Mech. Mutagen. (2009), doi:10.1016/j.mrfmmm.2009.02.001

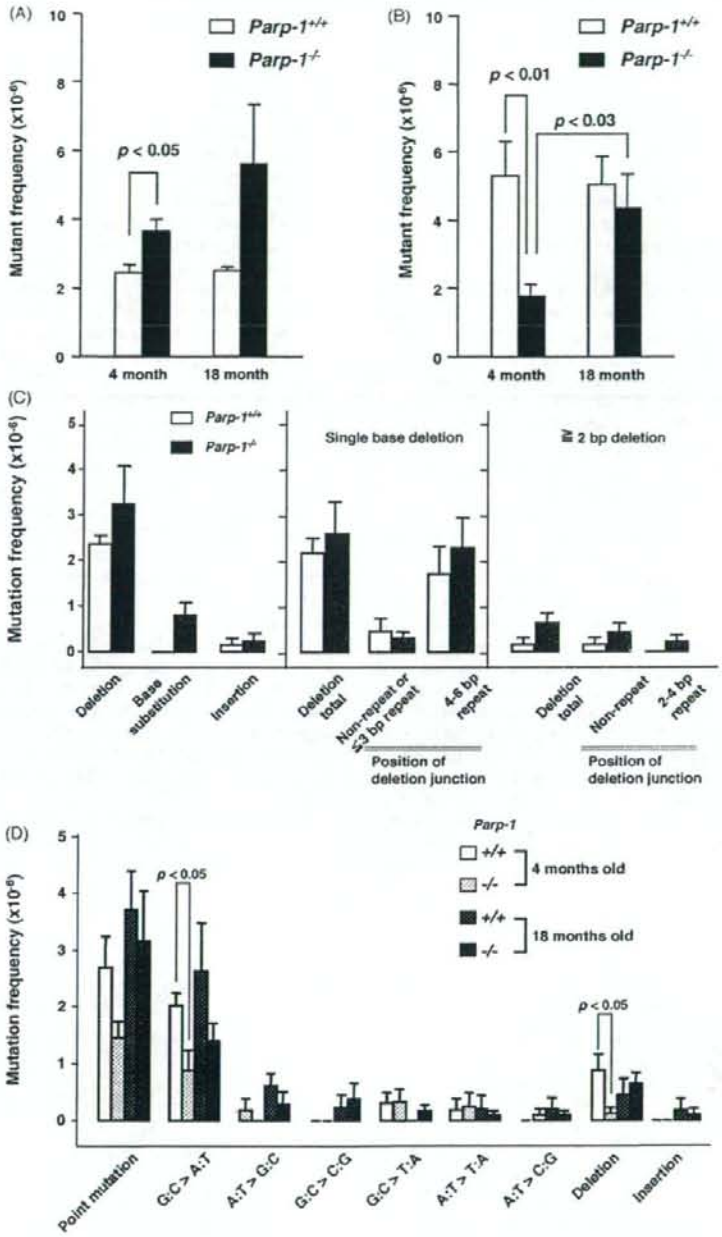

Fig. 2. Spontaneous mutant frequencies of the *red/gam* and *gpt* genes in the brain of *Parp-1*$^{-/-}$ and *Parp-1*$^{+/+}$ mice at 4 and 18 months of age. (A) Spontaneous mutant frequencies of the *red/gam* genes. (B) Spontaneous mutant frequencies in the *gpt* genes. Error bars represent standard error values. (C) Mutation spectra of the *red/gam* genes in the brain of *Parp-1*$^{-/-}$ and *Parp-1*$^{+/+}$ mice at 18 months of age. (D) Mutation spectra of the *gpt* genes in the brain of *Parp-1*$^{-/-}$ and *Parp-1*$^{+/+}$ mice at 4 and 18 months of age.

of *gpt* delta transgenic mice of mixed genetic background of SWR and C57BL/6 is reported to be 2.5×10^{-5} [22], which is higher compared to other reports on *gpt* delta mice [23,24]. This difference could be due to the mouse strain, tissues or other factors. From 4 to 18 months of age, the mutant frequency of the *gpt* gene in *Parp-1*$^{+/+}$ mice increased 2-fold. The mutant frequency of the *lacZ* marker gene in the liver is around 5×10^{-6} at 4–6 months of age and 1.2×10^{-5} at 24–34 months of age in wild-type mice [19]. Therefore age-dependent 2-fold increase in mutant frequency is consistently observed both in the *gpt* and *lacZ* [19] genes. On the other hand, size change mutations in the liver detected by the *lacZ* gene system did not significantly increase before 25–27 months [19] but

Please cite this article in press as: A. Shibata, et al., Role of Parp-1 in suppressing spontaneous deletion mutation in the liver and brain of mice at adolescence and advanced age, Mutat. Res.: Fundam. Mol. Mech. Mutagen. (2009), doi:10.1016/j.mrfmmm.2009.02.001

increased thereafter. Increase of mutant frequency in the *red/gam* gene in *Parp-1*$^{+/+}$ mice at 18 months of age, which detects deletion mutation, was not observed in the liver, being consistent with the results in the *lacZ* gene [19]. In the *lacZ* gene system, the target size is around 3000 bp, whereas that in the *gpt* and *red/gam* gene (Spi$^-$ assay) are around 456 and 417 bp, respectively. The smaller size of the target sequences of the *gpt* and *red/gam* genes could be also responsible for the lower spontaneous mutant frequencies.

In this study, *Parp-1*$^{-/-}$ mice showed a tendency of higher frequencies of spontaneous deletion mutations in the *red/gam* gene, including complex-type deletions in the liver ($p = 0.20$) and brain ($p = 0.29$) at 18 months of age.

The single base deletion mutations at non-repeat or short repeat sequences of the *red/gam* gene showed a 5.8-fold increase ($p = 0.031$) in the liver of *Parp-1*$^{-/-}$ mice compared to *Parp-1*$^{+/+}$ mice at 18 months of age. The frequency of deletion mutations of two bases or more also showed a 3.2-fold higher tendency in the *Parp-1*$^{-/-}$ than in the *Parp-1*$^{+/+}$ liver ($p = 0.084$). We observed complex-type deletions in the livers and brains of *Parp-1*$^{-/-}$ but not in *Parp-1*$^{+/+}$ mice at 18 months old.

8-Oxodeoxyguanosine (8-oxodG) is one outcome of major oxidative DNA damage [31]. The 8-oxodG levels in DNA of the liver, lungs, and small intestine in double knockout mice lacking both 8-oxoguanine DNA glycosylase 1 (*Ogg1*) and Mut Y homologue (*Myh*) genes increased linearly between 4 and 14 months of age [32]. 8-OxodG and SSB, which are expected outcomes of major endogenous DNA damage, are preferentially repaired by BER. Parp-1 is shown to be involved in BER and deletion mutations of single base and larger sizes of deletion as well as complexed-type were increased in *Parp-1*$^{-/-}$ mice after treatment with an alkylating agent, BHP [20]. The frequency of single base deletion mutations at non-repeat or short repeat sequences of the *red/gam* gene also increased 2.9-fold in *Parp-1*$^{-/-}$ mice compared to *Parp-1*$^{+/+}$ mice ($p = 0.043$) in the liver after treatment of the alkylating agent, whereas no difference in the frequency of single base deletion at 4–6 bp of mononucleotide repeats was observed between genotypes [20]. Therefore the spectra of single base deletions in the liver of *Parp-1*$^{-/-}$ mice at advanced age and after treatment with the alkylating agent are similar to each other. Stalled BER in the absence of Parp-1 at a SSB introduced step may further cause deletion mutations after treatment with an alkylating agent [20]. Therefore, there is a possibility that deletion mutation is also caused through BER induced by endogenous DNA damage during aging in *Parp-1*$^{-/-}$ mice. After introduction of SSB during BER, lack of Parp-1 may induce stall or delay in BER and terminal nucleotides may be destabilized and lost under *Parp-1* deficiency by exonuclease activity (Fig. 3). Collision between SSB and replication forks induces double strand breaks (DSBs) [33]. Two SSBs on opposite strands within at least 30 nt could resolve into a DSB [34]. Therefore, an increase of spontaneous DSBs might also be caused by the presence of SSBs during replication fork progression or defective BER under *Parp-1* deficiency.

Deletion mutations including single base deletions may be also produced during imprecise non-homologous end joining (NHEJ). In NHEJ reconstituted systems that utilize DSB substrates, it is shown that deletion or insertion of single bases as well as larger sizes occurs during the NHEJ process [35–37]. In chicken DT-40 cells, Parp-1 negatively regulates the NHEJ process by inhibiting Ku70/Ku80 action, and *Parp-1* deficiency causes an increase of NHEJ frequency [38]. However, DT-40 cells are known to have high HR levels compared to typical mammalian somatic cells. Using mouse embryonic fibroblast or CHO cells, it is demonstrated that Parp-1 competes with Ku for DSB binding and is shown to be involved in a backup pathway of classical NHEJ pathway with DNA ligase III [39]. Therefore, as shown in Fig. 3, during a NHEJ process of DSB, terminal nucleotides may be destabilized in the absence of Parp-1, and resection of bases by the exonuclease may lead to deletion mutation.

It is also notable that the frequency of single base deletions at 4–6 bp mononucleotide repeats did not show a difference between either genotypes in the livers and brains. Single base deletion mutations at 4–6 bp of mononucleotide repeats, namely at run sequences, might be caused by slippage error during DNA replication or repair reaction. The results suggest that Parp-1 is not essential to suppress these slippage type errors induced during aging.

Two complex-type deletions observed in *Parp-1*$^{-/-}$ mice accompanied small insertions as well as microhomologous sequences at deletion junctions, suggesting that these mutations could be

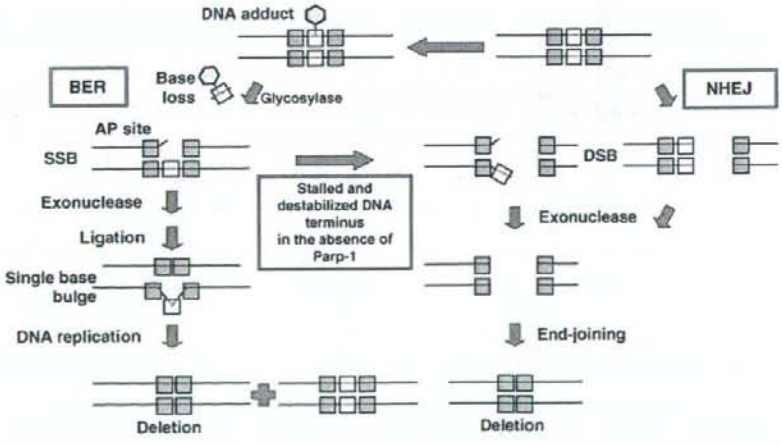

Fig. 3. A model for augmented development of deletion mutation through imprecise BER or NHEJ process in the absence of Parp-1. During BER, after single strand breaks are introduced following damaged base removal, the DNA terminus may be destabilized in the absence of Parp-1. Base loss could occur by the DNA exonuclease activity. When misannealing and ligation occur, the deletion will be fixed by subsequent DNA replication. Stalled BER reaction in the absence of Parp-1 on single strand breaks may also cause DSB and may induce switching to a NHEJ reaction and subsequently base loss will be fixed by end-joining process. During DSB repair process by NHEJ, base loss frequency might be augmented at the destabilized DNA terminus in the absence of Parp-1.

Please cite this article in press as: A. Shibata, et al., Role of Parp-1 in suppressing spontaneous deletion mutation in the liver and brain of mice at adolescence and advanced age, Mutat. Res.: Fundam. Mol. Mech. Mutagen. (2009), doi:10.1016/j.mrfmmm.2009.02.001

caused by insertion of a few nucleotides during microhomologous end-joining (MEJ)-type reactions. A few complementary bases are present at the 5′ position of the microhomologous sequences (marked with upper lines in Table 2). During the end-joining process, after resection of strand ends, transient base-pairing at microhomologous sequences may occur and a few complementary bases at the 5′ position may also form base-pairing. In the absence of Parp-1, these base-pairings may be destabilized and resection and insertion of a few bases may tend to occur in the livers. Consistently of all seven simple-type deletions of two bases or more observed in the livers of *Parp-1*$^{-/-}$ mice (Table 1), none harbored a few complementary bases at the 5′ position of the microhomologous sequences (data not shown). On the other hand, in two simple-type deletions of two bases or more in *Parp-1*$^{+/+}$ mice, one deletion harbored a few complementary bases at the 5′ position of the microhomologous deletion junctions (Table 1).

In the brain, one out of three complex-type deletions of *Parp-1*$^{-/-}$ mice harbored microhomologous deletion junctions but did not harbor complementary bases at 5′ positions of the microhomologous deletion junctions. This point should be further evaluated by analyzing deletion mutations induced after treatment with various types of DNA damaging agents in different tissues.

The xeroderma pigmentosum complementation group A (Xpa) plays an important role in nucleotide excision repair (NER) and *Xpa*-deficient mice also show higher spontaneous mutant frequencies in the liver at advanced ages [40]. In fact, *Xpa*-deficient mice show an increased frequency of hepatocellular adenomas at older ages [34]. It is thus possible that endogenous DNA damage repairable by NER may occur during aging. However, no increase in the susceptibility to carcinogenesis induced in *Parp-1*$^{-/-}$ mice by 4-nitrosoquinoline1-oxide [41], which induces bulky DNA adducts, suggests that Parp-1 is not involved in NER.

Most liver cells stay in the G0 phase and they usually enter the cell division cycle after various stimulating events. An augmented frequency of DNA replication, like that in preneoplastic lesions, can also increase the chance of DSBs and may increase the frequency of deletions. Two of six *Parp-1*$^{-/-}$ mice used in the mutation analysis harbored tumors in the liver and the tumor regions were not included for DNA isolation. Because the frequencies and spectrum of mutations in the *gpt* or *red/gam* genes were unbiased in each mouse, we can exclude the possibility that the tissues used for isolation of DNA contained monoclonally proliferating preneoplastic lesions or other cycling cells.

It is also possible that an increased frequency of cell division may be causative of augmented frequency of DSBs and may result in a higher frequency of deletion mutation. However, if this is true, the observed mutation spectrum is expected to be the same between the genotypes. We could rule out this possibility because we observed different spectra of deletion mutations between the genotypes.

Unexpectedly we also found a 3-fold lower frequency of point mutations in adolescent *Parp-1*$^{-/-}$ compared to *Parp-1*$^{+/+}$ mice in the brain ($p = 0.009$). An age-dependent increase in the mutant frequency in *Parp-1*$^{-/-}$ mice was also shown ($p = 0.011$). Lower frequencies of G:C to A:T type mutation and deletion mutation in *Parp-1*$^{-/-}$ mice suggest that Parp-1 may be positively involved imprecise repair pathways which cause base substitution mutation of G:C to A:T and deletion mutation in the brain.

In conclusion, this result supports the view that Parp-1 is involved in suppressing imprecise repair of endogenous DNA damage leading to deletion mutation during aging in the liver and brain. *Parp-1*$^{-/-}$ mice show increased incidence of hepatocellular tumors at 18–24 months of ages [13]. The present results suggest a substantial role of Parp-1 in the maintenance of genomic stability and suppression of carcinogenesis during aging.

Conflict of interest

The authors declare that there are no conflicts of interest.

Acknowledgements

We are grateful to M. Abe for technical assistance, M. Yanagihara for maintenance of the animals and H. Suzuki and S. Gotoh for helpful suggestions on the manuscript. This work was supported in part by a Grant-in-Aid for the Cancer Research from the Ministry of Health, Labour and Welfare, a Grand-in-Aid from Third Term Comprehensive 10-Year Strategy for Cancer Control, and a Grant-in-Aid for Scientific Research from the Ministry of Education, Science, Sports, and Culture of Japan (16-11804).

References

[1] M. Masson, C. Niedergang, V. Schreiber, S. Muller, J. Menissier-de Murcia, G. de Murcia, XRCC1 is specifically associated with poly(ADP-ribose) polymerase and negatively regulates its activity following DNA damage, Mol. Cell. Biol. 18 (1998) 3563–3571.
[2] C. von Kobbe, J.A. Harrigan, V. Schreiber, P. Stiegler, J. Piotrowski, L. Dawut, V.A. Bohr, Poly(ADP-ribose) polymerase 1 regulates both the exonuclease and helicase activities of the Werner syndrome protein, Nucleic Acids Res. 32 (2004) 4003–4014.
[3] C. von Kobbe, J.A. Harrigan, A. May, P.L. Opresko, L. Dawut, W.H. Cheng, V.A. Bohr, Central role for the Werner syndrome protein/poly(ADP-ribose) polymerase 1 complex in the poly(ADP-ribosyl)ation pathway after DNA damage, Mol. Cell. Biol. 23 (2003) 8601–8613.
[4] S. Galande, T. Kohwi-Shigematsu, Poly(ADP-ribose) polymerase and Ku autoantigen form a complex and synergistically bind to matrix attachment sequences, J. Biol. Chem. 274 (1999) 20521–20528.
[5] B. Li, S. Navarro, N. Kasahara, L. Comai, Identification and biochemical characterization of a Werner's syndrome protein complex with Ku70/80 and poly(ADP-ribose) polymerase-1, J. Biol. Chem. 279 (2004) 13659–13667.
[6] L. Lan, S. Nakajima, Y. Oohata, M. Takao, S. Okano, M. Masutani, S.H. Wilson, A. Yasui, In situ analysis of repair processes for oxidative DNA damage in mammalian cells, Proc. Natl. Acad. Sci. U.S.A. 101 (2004) 13738–13743.
[7] S. Okano, L. Lan, K.W. Caldecott, T. Mori, A. Yasui, Spatial and temporal cellular responses to single-strand breaks in human cells, Mol. Cell. Biol. 23 (2003) 3974–3981.
[8] F. Le Page, V. Schreiber, C. Dherin, G. De Murcia, S. Boiteux, Poly(ADP-ribose) polymerase-1 (PARP-1) is required in murine cell lines for base excision repair of oxidative DNA damage in the absence of DNA polymerase beta, J. Biol. Chem. 278 (2003) 18471–18477.
[9] J.B. Leppard, Z. Dong, Z.B. Mackey, A.E. Tomkinson, Physical and functional interaction between DNA ligase IIIalpha and poly(ADP-Ribose) polymerase 1 in DNA single-strand break repair, Mol. Cell. Biol. 23 (2003) 5919–5927.
[10] M. Tsutsumi, M. Masutani, T. Nozaki, O. Kusuoka, T. Tsujiuchi, H. Nakagama, H. Suzuki, Y. Konishi, T. Sugimura, Increased susceptibility of poly(ADP-ribose) polymerase-1 knockout mice to nitrosamine carcinogenicity, Carcinogenesis 22 (2001) 1–3.
[11] T. Nozaki, H. Fujihara, M. Watanabe, M. Tsutsumi, K. Nakamoto, O. Kusuoka, N. Kamada, H. Suzuki, H. Nakagama, T. Sugimura, M. Masutani, *Parp-1* deficiency implicated in colon and liver tumorigenesis induced by azoxymethane, Cancer Sci. 94 (2003) 497–500.
[12] A. Gunji, A. Uemura, M. Tsutsumi, T. Nozaki, O. Kusuoka, K. Omura, H. Suzuki, H. Nakagama, T. Sugimura, M. Masutani, *Parp-1* deficiency does not increase the frequency of tumors in the oral cavity and esophagus of ICR/129Sv mice by 4-nitroquinoline 1-oxide, a carcinogen producing bulky adducts, Cancer Lett. 241 (2005) 87–92.
[13] W.M. Tong, U. Cortes, M.P. Hande, H. Ohgaki, L.R. Cavalli, P.M. Lansdorp, B.R. Haddad, Z.Q. Wang, Synergistic role of Ku80 and poly(ADP-ribose) polymerase in suppressing chromosomal aberrations and liver cancer formation, Cancer Res. 62 (2002) 6990–6996.
[14] W.M. Tong, U. Cortes, Z.Q. Wang, Poly(ADP-ribose) polymerase: a guardian angel protecting the genome and suppressing tumorigenesis, Biochim. Biophys. Acta 1552 (2001) 27–37.
[15] W.M. Tong, H. Ohgaki, H. Huang, C. Granier, P. Kleihues, Z.Q. Wang, Null mutation of DNA strand break-binding molecule poly(ADP-ribose) polymerase causes medulloblastomas in p53(−/−) mice, Am. J. Pathol. 162 (2003) 343–352.
[16] M.E. Dolle, W.K. Snyder, J.A. Gossen, P.H. Lohman, J. Vijg, Distinct spectra of somatic mutations accumulated with age in mouse heart and small intestine, Proc. Natl. Acad. Sci. U.S.A. 97 (2000) 8403–8408.
[17] K.A. Hill, V.L. Buettner, A. Halangoda, M. Kunishige, S.R. Moore, J. Longmate, W.A. Scaringe, S.S. Sommer, Spontaneous mutation in Big Blue mice from fetus to old age: tissue-specific time courses of mutation frequency but similar mutation types, Environ. Mol. Mutagen. 43 (2004) 110–120.
[18] T. Ono, H. Ikehata, S. Nakamura, Y. Saito, Y. Hosoi, Y. Takai, S. Yamada, J. Onodera, K. Yamamoto, Age-associated increase of spontaneous mutant frequency and

molecular nature of mutation in newborn and old lacZ-transgenic mouse, Mutat. Res. 447 (2000) 165–177.
[19] M.E. Dolle, H. Giese, C.L. Hopkins, H.J. Martus, J.M. Hausdorff, J. Vijg, Rapid accumulation of genome rearrangements in liver but not in brain of old mice, Nat. Genet. 17 (1997) 431–434.
[20] A. Shibata, N. Kamada, K. Masumura, T. Nohmi, S. Kobayashi, H. Teraoka, H. Nakagama, T. Sugimura, H. Suzuki, M. Masutani, *Parp-1* deficiency causes an increase of deletion mutations and insertions/rearrangements in vivo after treatment with an alkylating agent, Oncogene 24 (2005) 1328–1337.
[21] T. Nohmi, M. Katoh, H. Suzuki, M. Matsui, M. Yamada, M. Watanabe, M. Suzuki, N. Horiya, O. Ueda, T. Shibuya, H. Ikeda, T. Sofuni, A new transgenic mouse mutagenesis test system using Spi- and 6-thioguanine selections, Environ. Mol. Mutagen. 28 (1996) 465–470.
[22] R.R. Swiger, L. Cosentino, K.I. Masumura, T. Nohmi, J.A. Heddle, Further characterization and validation of gpt delta transgenic mice for quantifying somatic mutations in vivo, Environ. Mol. Mutagen. 37 (2001) 297–303.
[23] K. Masumura, K. Kuniya, T. Kurobe, M. Fukuoka, F. Yatagai, T. Nohmi, Heavy-ion-induced mutations in the *gpt* delta transgenic mouse: comparison of mutation spectra induced by heavy-ion, X-ray, and gamma-ray radiation, Environ. Mol. Mutagen. 40 (2002) 207–215.
[24] K. Masumura, T. Nohmi, Spontaneous mutagenesis in rodents: spontaneous gene mutations identified by neutral reporter genes in *gpt* delta transgenic mice and rats, J. Health Sci. 55 (2009) 40–49.
[25] K. Masumura, K. Matsui, M. Yamada, M. Horiguchi, K. Ishida, M. Watanabe, O. Ueda, H. Suzuki, Y. Kanke, K.R. Tindall, K. Wakabayashi, T. Sofuni, T. Nohmi, Mutagenicity of 2-amino-1-methyl-6-phenylimidazo [4,5-b]pyridine (PhIP) in the new *gpt* delta transgenic mouse, Cancer Lett. 143 (1999) 241–244.
[26] F. Yatagai, T. Kurobe, T. Nohmi, K. Masumura, T. Tsukada, H. Yamaguchi, K. Kasai-Eguchi, N. Fukunishi, Heavy-ion-induced mutations in the gpt delta transgenic mouse: effect of p53 gene knockout, Environ. Mol. Mutagen. 40 (2002) 216–225.
[27] A. Shibata, M. Masutani, T. Nozaki, N. Kamada, H. Fujihara, K. Masumura, H. Nakagama, T. Sugimura, S. Kobayashi, H. Suzuki, T. Nohmi, Improvement of the Spi-assay for mutations in *gpt* delta mice by including magnesium ions during plaque formation, Environ. Mol. Mutagen. 41 (2003) 370–372.
[28] T. Nohmi, M. Suzuki, K. Masumura, M. Yamada, K. Matsui, O. Ueda, H. Suzuki, M. Katoh, H. Ikeda, T. Sofuni, Spi(-) selection: an efficient method to detect gamma-ray-induced deletions in transgenic mice, Environ. Mol. Mutagen. 34 (1999) 9–15.
[29] A. Shibata, M. Masutani, N. Kamada, K. Masumura, H. Nakagama, S. Kobayashi, H. Teraoka, H. Suzuki, T. Nohmi, Efficient method for mapping and characterizing structures of deletion mutations in *gpt* delta mice using Southern blot analysis with oligo DNA probes, Environ. Mol. Mutagen. 43 (2004) 204–207.
[30] K. Masumura, M. Matsui, M. Katoh, N. Horiya, O. Ueda, H. Tanabe, M. Yamada, H. Suzuki, T. Sofuni, T. Nohmi, Spectra of *gpt* mutations in ethylnitrosourea-treated and untreated transgenic mice, Environ. Mol. Mutagen. 34 (1999) 1–8.
[31] H. Kasai, P.F. Crain, Y. Kuchino, S. Nishimura, A. Ootsuyama, H. Tanooka, Formation of 8-hydroxyguanine moiety in cellular DNA by agents producing oxygen radicals and evidence for its repair, Carcinogenesis 7 (1986) 1849–1851.
[32] M.T. Russo, G. De Luca, P. Degan, E. Parlanti, E. Dogliotti, D.E. Barnes, T. Lindahl, H. Yang, J.H. Miller, M. Bignami, Accumulation of the oxidative base lesion 8-hydroxyguanine in DNA of tumor-prone mice defective in both the *Myh* and *Ogg1* DNA glycosylases, Cancer Res. 64 (2004) 4411–4414.
[33] T. Furuta, H. Takemura, Z.Y. Liao, G.J. Aune, C. Redon, O.A. Sedelnikova, D.R. Pilch, E.P. Rogakou, A. Celeste, H.T. Chen, A. Nussenzweig, M.I. Aladjem, W.M. Bonner, Y. Pommier, Phosphorylation of histone H2AX and activation of Mre11, Rad50, and Nbs1 in response to replication-dependent DNA double-strand breaks induced by mammalian DNA topoisomerase I cleavage complexes, J. Biol. Chem. 278 (2003) 20303–20312.
[34] S. Vispe, M.S. Satoh, DNA repair patch-mediated double strand DNA break formation in human cells, J. Biol. Chem. 275 (2000) 27386–27392.
[35] F. Liang, M. Han, P.J. Romanienko, M. Jasin, Homology-directed repair is a major double-strand break repair pathway in mammalian cells, Proc. Natl. Acad. Sci. U.S.A. 95 (1998) 5172–5177.
[36] M. Honma, M. Sakuraba, T. Koizumi, Y. Takashima, H. Sakamoto, M. Hayashi, Non-homologous end-joining for repairing I-SceI-induced DNA double strand breaks in human cells, DNA Repair (Amst.) 6 (2007) 781–788.
[37] Y. Ma, H. Lu, B. Tippin, M.F. Goodman, N. Shimazaki, O. Koiwai, C.L. Hsieh, K. Schwarz, M.R. Lieber, A biochemically defined system for mammalian nonhomologous DNA end joining, Mol. Cell 16 (2004) 701–713.
[38] H. Hochegger, D. Dejsuphong, T. Fukushima, C. Morrison, E. Sonoda, V. Schreiber, G.Y. Zhao, A. Saberi, M. Masutani, N. Adachi, H. Koyama, G. de Murcia, S. Takeda, Parp-1 protects homologous recombination from interference by Ku and Ligase IV in vertebrate cells, EMBO J. 25 (2006) 1305–1314.
[39] M. Wang, W. Wu, W. Wu, B. Rosidi, L. Zhang, H. Wang, G. Iliakis, PARP-1 and Ku compete for repair of DNA double strand breaks by distinct NHEJ pathways, Nucleic Acids Res. 34 (2006) 6170–6182.
[40] H. Giese, M.E. Dolle, A. Hezel, H. van Steeg, J. Vijg, Accelerated accumulation of somatic mutations in mice deficient in the nucleotide excision repair gene *XPA*, Oncogene 18 (1999) 1257–1260.
[41] A. de Vries, C.T. van Oostrom, P.M. Dortant, R.B. Beems, C.F. van Kreijl, P.J. Capel, H. van Steeg, Spontaneous liver tumors and benzo[a]pyrene-induced lymphomas in *XPA*-deficient mice, Mol. Carcinogen. 19 (1997) 46–53.

Please cite this article in press as: A. Shibata, et al., Role of Parp-1 in suppressing spontaneous deletion mutation in the liver and brain of mice at adolescence and advanced age, Mutat. Res.: Fundam. Mol. Mech. Mutagen. (2009), doi:10.1016/j.mrfmmm.2009.02.001

Genes and Environment, Vol. 31, No. 1 pp. 1–8 (2009)

Regular article

In Vivo Mutagenesis Caused by Diesel Exhaust in the Testis of *gpt* delta Transgenic Mice

Akiko H. Hashimoto[1], Kimiko Amanuma[1], Kenichi Masumura[2], Takehiko Nohmi[2] and Yasunobu Aoki[1,3]

[1]Research Center for Environmental Risk, National Institute for Environmental Studies, Ibaraki, Japan
[2]Division of Genetics and Mutagenesis, National Institute of Health Sciences, Tokyo, Japan

(Received June 30, 2008; Revised August 11, 2008; Accepted August 20, 2008)

Diesel exhaust (DE) is a major airborne pollutant in urban areas. In this study, we estimated the systemic effect of diesel exhaust inhalation by investigating mutations in extraplumonary organs such as the testis and liver. *gpt* delta Transgenic mice carrying the guanine phosphoribosyltransferase (*gpt*) transgene for the detection of mutations in genomic DNA were exposed to inhalation of 3 mg m^{-3} diesel exhaust (as suspended particulate matter) for 12 or 24 weeks. Compared to the control mice, DE resulted in a 2.0-fold increase in mutant frequency in the testis of mice that were exposed to DE for 24 weeks (inhaled group, 1.17×10^{-5}; control group, 0.57×10^{-5}), but not in the testis of mice exposed for 12 weeks (0.61×10^{-5}). The mutant frequency in the lungs was 2.6-fold higher in mice exposed to DE for 24 weeks than the control group, but it was not elevated in the liver (0.67×10^{-5}). In the testis, the major mutations on the *gpt* gene were G:C→T:A transversions, 1 base deletions and G:C→A:T transitions, while the major mutation in the lung was G:C→A:T transitions. The mutations on nucleotide nos. 402, 406, 409 and 416–418 in the *gpt* gene in testis seemed to be characteristic of DE inhalation in the testis. Our results suggest that inhalation of diesel exhaust is genotoxic to the testis as well as respiratory organs.

Key words: diesel exhaust emission, testis, *gpt* delta transgenic mouse, 6-thioguanine selection

Introduction

Diesel exhaust (DE) emission is a major source of air pollutant in urban areas, and has been implicated in causing allergic respiratory disease and lung cancer (1,2). Diesel exhaust particles (DEP) have been known to contain potent carcinogens and mutagens, such as polyaromatic hydrocarbons (PAH; e.g., benzo[*a*]pyrene (B[*a*]P)) and nitrated PAH (e.g., 1,6-dinitropyrene (1,6-DNP)), of which mutagenicity has been evaluated *in vitro* using a *Salmonella typhimurium* TA98 assay (3,4). Exposure to DEP through inhalation or intratracheal instillation have been shown to cause oxidative DNA damage (5,6) and DNA adduct formation (7,8) in rat and mouse lungs, and long periods of inhalation of DE resulted in respiratory tract tumors in rats (9–12). These observations suggest that mutagens in DE induce mutations in the lung, a primary target organ of inhalation, and are responsible for inducing lung cancer. Furthermore, we have previously demonstrated that typical mutagens such as B[*a*]P (13) and 1,6-DNP (14), as well as inhalation of DE (15,16), caused mutations in the lungs using transgenic rodents for analyzing *in vivo* mutagenesis (Big Blue® rat and *gpt* delta mouse). Metabolites of PAH contained in suspended particulate matter in ambient air have been detected in human urine (17), suggesting that mutagenic PAH in DE are absorbed in the lungs and transported to extrapulmonary organs, such as the testis and liver, where they could exert possible genotoxicity. Watanabe *et al.* showed that the number of daily sperm and Sertoli cells in fetuses and male rats was decreased by DE exposure (18,19). However, the mutagenic effect of DE on the extrapulmonary organs has remained unclear.

We intended to evaluate the *in vivo* mutagenicity of DE in testis and liver to obtain fundamental data for assessing the health risks of air pollution. In order to evaluate *in vivo* mutagenicity, we used the *gpt* delta transgenic mice carrying the lambda phage EG10 as a transgene for detecting mutations on genomic DNA (20,21). When the rescued phage is infected into *E. coli* expressing Cre recombinase, the phage DNA is converted into plasmids harboring the chloramphenicol (Cm)-resistance gene and guanine phosphoribosyltransferase (*gpt*) gene. The *gpt* mutants can be positively detected as colonies arising on plates containing Cm and 6-thioguanine (6-TG). Our study revealed an elevated mutant frequency and alterations in the mutation spectrum in the testis of DE-inhaled *gpt* delta transgenic mice in which

[3]Correspondence to: Yasunobu Aoki, Research Center for Environmental Risk, National Institute for Environmental Studies, 16-2 Onogawa, Tsukuba, Ibaraki 305-8506, Japan. Tel: +81-29-850-2390, Fax: +81-29-850-2588, E-mail: ybaoki@nies.go.jp

the mutant frequency in the lung has already been reported to increase (16).

In this study, we show that inhalation of 3 mg m^{-3} DE (as suspended particulate matter (SPM)) for 24 weeks resulted in a 2.0-fold increase in mutant frequency in the testis of *gpt* delta mice compared to the controls, but the inhalation for 12 weeks did not elevate the mutant frequency in the testis. The mutant frequency in the liver was not increased by inhalation of DE under conditions where the mutant frequency in the testis and lungs were significantly increased. The predominant mutation spectrum in the testis in response to DE inhalation included G:C→T:A transversions, 1-base deletions and G:C→A:T transitions, while the major mutations in the lungs were G:C→A:T transitions (16). These data suggest that DE inhalation exerts genotoxicity on testis systemically.

Materials and Methods

Treatment of mice: *gpt* delta Mice carry ca. 80 copies of lambda EG10 DNA on each chromosome 17 in a C57BL/6J background (22). Exposure to DE (12 h d^{-1}, 7 d $week^{-1}$) was performed in chambers equipped by the National Institute for Environmental Studies (16,23) under the same conditions as those in our previous report on *in vivo* mutations in the lung (16). Three to five 7-week-old mice were exposed to 3 mg m^{-3} DE (as SPM) for 12 or 24 weeks. Seven mice were maintained in filtered clean air (control group). The animals were sacrificed 3 days after the last exposure and their testis and liver were removed, frozen in liquid nitrogen and stored at −80°C for this study.

***Gpt* mutation assay:** The *gpt* assay was performed as described previously (20). Genomic DNA was extracted from the testis and liver tissue using the RecoverEase DNA Isolation Kit (Stratagene Co., La Jolla, CA) and Lambda EG10 phages were rescued using the Transpack® Packaging Extract (Stratagene). *E. coli* YG6020 was infected with the phage, spread on M9 salt plates containing Cm and 6-TG (19), and then incubated for 72 h at 37°C for selection of the colonies harboring a plasmid carrying the chloramphenicol acetyltransferase (CAT) gene and a mutated *gpt* gene. Isolates from the 6-TG-resistant phenotype were cultured in LB broth containing 25 $\mu g/mL^{-1}$ Cm at 37°C overnight, harvested by centrifugation (7,000 rpm, 10 min) and stored at −80°C.

PCR and DNA sequencing of the 6-TG-resistant mutants: A 739 bp DNA fragment containing the *gpt* gene was amplified by PCR and sequenced as described previously (13,20). Sequencing was performed using the Big Dye Terminator v3.1 Cycle Sequencing Kit (Applied Biosystems, Foster City, CA) on an Applied Biosystems model 3730xl DNA analyzer.

Statistical analysis: All of the data are expressed as the mean ± SD. The statistical significance of the DE treatment was analyzed using the Student's *t*-test. $p<0.05$ was considered to be statistically significant. Mutational spectra were compared using the Adams-Skopek test (24,25).

Results

***Gpt* mutations in the testis, lung and liver of DE inhaled *gpt* delta mice:** In order to estimate the mutagenicity of DE, *gpt* delta mice inhaled DE (3 mg m^{-3} as SPM) for 12 or 24 weeks and mutations in the testis and liver were analyzed (Table 1). While the mutant frequencies in the testis of the control mice for 12 and 24 weeks inhalation were $0.57 \pm 0.04 \times 10^{-5}$ and $0.58 \pm 0.07 \times 10^{-5}$, respectively, inhalation of DE for 12 and 24 weeks resulted in 1.1 and 2.0-fold increases in mutant frequency ($0.61 \pm 0.08 \times 10^{-5}$ and $1.17 \pm 0.45 \times 10^{-5}$, respectively) compared with the controls (Table 1). Significant increases in the mutant frequency in the testis were observed in the group that inhaled DE for 24 weeks compared with the control group and the group that inhaled DE for 12 weeks. Our previous report demonstrated that inhalation of 3 mg m^{-3} DE for 24 weeks resulted in a 2.6-fold increase in the mutant frequency in the lung (Table 1) (16); however, the mutant frequency in the liver ($0.67 \pm 0.23 \times 10^{-5}$) was not elevated even after inhalation for 24 weeks compared with the control ($0.56 \pm 0.14 \times 10^{-5}$).

Alterations in the mutation spectrum in testis are induced by DE inhalation: In order to determine the mutation spectrum induced by DE inhalation, 170 6-TG-resistant mutants in a total were sequenced. As shown in Table 2, mutations of the *gpt* gene were detected in 149 mutants obtained from the testis of DE-inhaled and control mice (Table 1). The mutation type analysis indicated that the percentages of G:C→T:A transversions and 1-base deletions were increased in DE-inhaled mice (DE all) comparing to control mice (Control all). To characterize DE-induced mutagenesis precisely, the frequency of each mutation was calculated from data in Table 2 (Fig. 1). In the groups that inhaled DE for 24 weeks, the mutant frequency of G:C→T:A transversions, 1-base deletions and G:C→A:T transitions was 3.8×10^{-6}, 2.9×10^{-6} and 2.4×10^{-6}, whereas that of the control mice was, 1.0×10^{-6}, 0.6×10^{-6} and 1.9×10^{-6}, respectively. DE inhalation for 24 weeks caused a significant difference in the types of mutation in the control and DE inhalation groups ($p=0.04$, Adams-Skopek test).

The spectrum of *gpt* mutations in the testis that were induced by DE inhalation for 12 weeks and 24 weeks (Table 3) indicated a prevalence of G:C→T:A transversions with three mutation sites (nucleotide nos. 402, 406 and 409) being identified as hotspots in three or more mice, as well as G:C→A:T transition hotspots on

Table 1. Summary of mutant frequencies in the testis, lung and liver of *gpt* delta mice after inhalation of DE

Organ	DE concentration (mg m^{-3})	Exposure time (weeks)	ID of animals	Number of colonies		Mutant frequency ($\times 10^{-5}$)	Average mutant frequency ± SD ($\times 10^{-5}$)
				Mutant	Total		
Testis	0	12	1	7	1,265,600	0.55	
			2	9	1,428,800	0.63	
			3	10	1,792,000	0.56	
			4	10	1,820,800	0.55	
			Total	36	6,307,200		0.57 ± 0.04
	3	12	1	12	1,996,800	0.60	
			2	12	1,984,800	0.61	
			3	14	1,881,600	0.74	
			4	14	2,318,400	0.60	
			5	7	1,374,400	0.51	
			Total	59	9,556,000		0.61 ± 0.08
	0	24	1	9	1,676,800	0.54	
			2	5	756,800	0.66	
			3	7	1,291,200	0.54	
			Total	21	3,724,800		0.58 ± 0.07
	3	24	1	9	1,409,600	0.64	
			2	29	1,910,400	1.52	
			3	16	1,176,000	1.36	
			Total	54	4,496,000		1.17 ± 0.45*
Lung†	0	24	1	13	1,551,000	0.84	
			2	8	1,074,000	0.74	
			3	8	903,000	0.89	
			Total	29	3,528,000		0.82 ± 0.07
	3	24	1	10	462,500	2.16	
			2	11	546,000	2.01	
			3	16	745,600	2.15	
			Total	37	1,754,100		2.11 ± 0.08**
Liver	0	24	1	4	952,000	0.42	
			2	8	1,148,800	0.70	
			3	4	724,800	0.55	
			Total	16	2,825,600		0.56 ± 0.14
	3	24	1	2	275,200	0.73	
			2	2	483,200	0.41	
			3	8	937,600	0.85	
			Total	12	1,696,000		0.67 ± 0.23

Significant differences were detected between the control and DE-treated group (*: $p<0.05$, **: $p<0.001$).
†: data from our previous study (16).

another three sites (nucleotide nos. 64, 110 and 115). The predominant frameshift mutations induced by DE were single-base pair deletions in run sequences (22/29 = 76%); in this case the hotspot was located at nucleotide nos. 416–418. Therefore, the mutations on nucleotide nos. 402, 406, 409 and 416–418 seem to be characteristic of DE inhalation in testis, but were not hotspots in the lungs of DE-inhaled mice, while nucleotide no. 402 was a hotspot of G:C→A:T transitions in the lung.

Discussion

In this study we demonstrate that, as a result of inhalation of 3 mg m^{-3} DE, the mutant frequency in the testis of *gpt* delta mice increased with the duration of treatment (Table 1), but the mutant frequency in the liver was not elevated, indicating that DE inhalation exerts genotoxicity systemically on testis as well as on respiratory organs. This article is the first report on an increase in the mutant frequency in testis in response to DE inhalation (Table 1). Indeed, DE inhalation has also been

Table 2. Classification of *gpt* mutations from the testis of control and DE-inhaled mice

Type of mutation in the *gpt* gene	Control (weeks)			DE (weeks)		
	12	24	all	12	24	all
	%			%		
Base substitution						
Transition						
G:C→A:T	42	31	39	24	24	24
A:T→G:C	6	6	6	2	4	3
Transversion						
G:C→T:A	12	38	20	24	37	30
G:C→C:G	12	6	10	17	0	9
A:T→T:A	3	0	2	2	2	2
A:T→C:G	0	0	0	0	2	1
Deletion						
−1	12	13	12	30	28	29
>2	6	6	6	0	2	1
Insertion	6	0	4	2	0	1
Other	0	0	0	0	0	0
Total	100	100	100	100	100	100
Total number of mutants*	33	16	49	54	46	100

*: 149 of 170 6-TG-resitant mutants have mutation in the *gpt* gene.

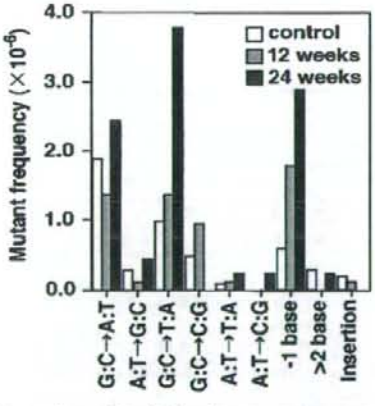

Fig. 1. Comparison of the 6-TG-resistant mutation spectra in control and DE inhaled *gpt* delta mice. The mutant frequencies of control mice and those exposed to DE for 12 weeks and 24 weeks were calculated by dividing the number of each type of *gpt* mutations in the Control all, DE 12 weeks and DE 24 weeks, respectively, by the corresponding total number of colonies (shown in Table 1).

shown to cause a decrease in the number of daily sperm and Sertoli cells in fetuses and male rats (18,19). Daily sperm production in the testis decreased dose-dependently in response to DE exposure for 6 months; a 53% reduction in sperm production was observed in rats exposed to DE (26) at the same concentration (3 mg m^{-3}) used in this study. These observations indicate that DE inhalation induces an increase in mutant frequency in the testis under the same conditions in which the reproduction of sperm was suppressed.

A significant increase in mutant frequency was observed in the testis after DE inhalation for 24 weeks but not for 12 weeks, while the mutant frequency in the lungs was elevated after inhalation for 24 weeks as well as 12 weeks (16). Delayed mutagenesis in germ cells has been observed in *lacZ* transgenic mice after 35 days treatment with ethyl nitrosourea (ENU) (27). Mutagens contained in DE were absorbed in the lung, systemically transported to the testis and possibly caused DNA adduct formation in spermatogonial stem cells and spermatogonia. These DNA adducts may be fixed as delayed mutations in germ cells through errors in DNA replication in continuous cell division during germ-cell development from spermatogenic cells to sperm. On the other hand, DNA adducts may be formed in the liver, but might not be fixed as mutations because of the low rate of cell division and/or high degree of DNA repair. However, Masumura *et al.* (28) showed that a heterocyclic amine, PhIP, was metabolically activated and induced point mutations in the liver but not the testis of *gpt* delta mice, suggesting that any factors governing the distribution and metabolism of mutagens in the body may determine the tissue specificity of mutagenesis.

The predominant mutation spectrum in the testis in response to DE included G:C→T:A transversions, 1-base deletions and G:C→A:T transitions (Table 2 and Fig. 1) as well as mutation hotspots on nucleotide nos. 402, 406 and 409, nos. 416–418 and nos. 64, 110 and 115, respectively (Table 3), while mutations in the lung were predominantly only G:C→A:T transitions (16). Mutation hotspots on nucleotide no. 406 and nos. 416–418 were identified in the testis of mice that inhaled DE for 12 weeks, in which the mutant frequency did not significantly increase, suggesting that DE acts as mutagenic agent even after inhalation for 12 weeks. G:C→T:A transversions have been known to be induced in *gpt* delta mice by B[*a*]P treatment (13) and 8-hydroxy-deoxyguanine (8-OHdG) generated by reactive oxygen species (ROS) (29). We have shown that the G:C→T:A transversion was a predominant mutation in Nrf2 deficient mice (30), in which the levels of the phase II detoxification enzymes and ROS-scavenging enzymes were suppressed (31,32) and DNA adduct formation was accelerated in the lung (33). These observations suggest some contribution of ROS to inducing mutation hotspots of G:C→T:A transversions (nucleotide nos. 402, 406 and 409) in the testis of mice subjected to DE inhalation. Nucleotide nos. 64, 110 and 115 were mutation hotspots of G:C→A:T transitions in the testis of DE-inhaled mice as well as in 1,6-dinitropyrene (DNP)-instilled lungs of *gpt* delta mice (14), and were also mutation hotspots in non-treated mice (34). The compo-

Table 3. DNA sequence analysis of *gpt* mutations obtained from the testis of DE-treated and control mice

Type of mutation	Mutation			Amino acid change			Number			
	Nucleotide number	Sequence Change					Control		DE	
							12 weeks	24 weeks	12 weeks	24 weeks
Base substitution										
Transition										
G:C→A:T	3	atG → atA		Met	→	Ile	1			
	64	Cga → Tga	CpG	Arg	→	Stop	1		4†	
	82	Caa → Taa		Gln	→	Stop	1			
	86	tGg → tAg		Trp	→	Stop	1			
	107	aGc → aAc		Ser	→	Asn		1		
	110	cGt → cAt	CpG	Arg	→	His	2*		2	2*
	113	gGc → gAc		Gly	→	Asp		1	1	
	115	Ggt → Agt	CpG	Gly	→	Ser	1		3*	3*
	116	gGt → gAt		Gly	→	Asp	2*	1	1	1
	145	Gaa → Aaa		Glu	→	Lys			1	
	176	tGt → tAt		Cys	→	Tyr	1			
	202	Cag → Tag		Gln	→	Stop				1
	401	tGg → tAg		Trp	→	Stop	1			
	402	tgG → tgA		Trp	→	Stop			1	1
	418	Gat → Aat		Asp	→	Asn	3†	1		3*
	451	Ggt → Agt	CpG	Gly	→	Ser		1		
A:T→G:C	56	cTc → cCc		Leu	→	Pro	1			1
	410	cAg → cGg		Gln	→	Arg				1
	415	Tgg → Cgg		Trp	→	Arg	1			
	419	gAt → gGt		Asp	→	Gly		1	1	
Transversion										
G:C→T:A	7	Gaa → Taa	CpG	Glu	→	Stop				1
	59	gCa → gAa		Ala	→	Glu				1
	110	cGt → cTt	CpG	Arg	→	Leu				1
	127	Ggt → Tgt		Gly	→	Cys				1
	140	gCg → gAg	CpG	Ala	→	Glu		2	1	1
	145	Gaa → Taa		Glu	→	Stop				1
	189	taC → taA	CpG	Tyr	→	Stop		1	1	
	208	Gag → Tag	CpG	Glu	→	Stop				1
	287	aCt → aAt		Thr	→	Asn			1	
	304	Gaa → Taa		Glu	→	Stop	1		1	1
	401	tGg → tTg		Trp	→	Leu	1			1
	402	tgG → tgT		Trp	→	Cys	1		2*	1
	406	Gaa → Taa		Glu	→	Stop			4†	4*
	409	Cag → Aag		Gln	→	Lys			1	2*
	413	cCg → cAg	CpG	Pro	→	Gln	1	2*		1
	418	Gat → Tat		Asp	→	Tyr		1	2*	
G:C→C:G	3	atG → atC		Met	→	Ile			1	
	6	agC → agG	CpG	Ser	→	Arg	1			
	109	Cgt → Ggt	CpG	Arg	→	Gly			1	
	143	cGt → cCt	CpG	Arg	→	Pro	1			
	145	Gaa → Caa		Glu	→	Gln			1	
	262	Gat → Cat		Asp	→	His	1			
	289	Gcg → Ccg		Ala	→	Pro			1	
	340	Gca → Cca	CpG	Ala	→	Pro			2*	
	401	tGg → tCg		Trp	→	Ser			1	
	402	tgG → tgC		Trp	→	Cys		1		
	413	cCg → cGg	CpG	Pro	→	Arg			2*	
	418	Gat → Cat		Asp	→	His	1			
A:T→T:A	35	tTg → tAg		Leu	→	Stop				1
	146	gAa → gTa		Glu	→	Val			1	
	179	aTt → aAt		Ile	→	Asn	1			
A:T→C:G	106	Agc → Cgc		Ser	→	Arg				1